

AD-A078 218

ARMY ARMAMENT RESEARCH AND DEVELOPMENT COMMAND ABERD--ETC F/G 20/8
THE THEORETICAL TREATMENT OF PARTICLE SWARMS.(U)

UNCLASSIFIED

SEP 79 R D SHELTON , A L ARBUCKLE
ARBRL-TR-02195

SBIE -AD-E430 336

NL

| OF |
ADA
078218



END
DATE
FILMED
1-80
DDC

AD-E 430 336

LEVEL

12

AD

AD A 078218

TECHNICAL REPORT ARBRL-TR-02195 ✓

THE THEORETICAL TREATMENT OF
PARTICLE SWARMS

R. D. Shelton
A. L. Arbuckle

DDC
RECEIVED
DEC 17 1979
E

September 1979

DDC FILE COPY



US ARMY ARMAMENT RESEARCH AND DEVELOPMENT COMMAND
BALLISTIC RESEARCH LABORATORY
ABERDEEN PROVING GROUND, MARYLAND

Approved for public release; distribution unlimited.

79 11 30 029

Destroy this report when it is no longer needed.
Do not return it to the originator.

Secondary distribution of this report by originating
or sponsoring activity is prohibited.

Additional copies of this report may be obtained
from the National Technical Information Service,
U.S. Department of Commerce, Springfield, Virginia
22151.

The findings in this report are not to be construed as
an official Department of the Army position, unless
so designated by other authorized documents.

*The use of trade names or manufacturers' names in this report
does not constitute indorsement of any commercial product.*

UNCLASSIFIED

SECURITY CLASSIFICATION OF THIS PAGE (When Data Entered)

REPORT DOCUMENTATION PAGE		READ INSTRUCTIONS BEFORE COMPLETING FORM
1. REPORT NUMBER 14 TECHNICAL REPORT ARBRL-TR-02195	2. GOVT ACCESSION NO.	3. RECIPIENT'S CATALOG NUMBER
4. TITLE (and Subtitle) 6 THE THEORETICAL TREATMENT OF PARTICLE SWARMS.	5. TYPE OF REPORT & PERIOD COVERED 9 Final rept.	
7. AUTHOR(s) 10 R. D. Shelton A. L. Arbuckle	8. CONTRACT OR GRANT NUMBER(s)	
9. PERFORMING ORGANIZATION NAME AND ADDRESS US Army Ballistic Research Laboratory ATTN: DRDAR-BLT Aberdeen Proving Ground, MD 21005	10. PROGRAM ELEMENT, PROJECT, TASK AREA & WORK UNIT NUMBERS 16 RDT&E IL162618AH80	
11. CONTROLLING OFFICE NAME AND ADDRESS US Army Armament Research and Development Command US Army Ballistic Research Laboratory ATTN: DRDAR-BL Aberdeen Proving Ground, MD 21005	12. REPORT DATE 11 SEPT 1979	13. NUMBER OF PAGES 65
14. MONITORING AGENCY NAME & ADDRESS (if different from Controlling Office) 12/65	15. SECURITY CLASS. (of this report) UNCLASSIFIED	
15a. DECLASSIFICATION/DOWNGRADING SCHEDULE		
16. DISTRIBUTION STATEMENT (of this Report) Approved for public release, distribution unlimited. 18 SBIE 19 AD-EH30 336		
17. DISTRIBUTION STATEMENT (of the abstract entered in Block 20, if different from Report)		
18. SUPPLEMENTARY NOTES		
19. KEY WORDS (Continue on reverse side if necessary and identify by block number) Liouville's theorem, Dirac delta function, particle distributions in general force fields, Schwarzschild field, meteoroids, charged particles, photons, stars		
20. ABSTRACT (Continue on reverse side if necessary and identify by block number) (K15) Particle swarms come into consideration when a group of independent particles move without collision in a force field such that a fluid Hamiltonian can be written to represent the motion. Typical problems from several fields are collected and united under a single theoretical framework. The fields include such problems as fragment distributions from an exploding warhead, micrometeoroid distributions in the vicinity of the earth, charged particle distributions in a magnetic bottle, focussing of photons by heavy stars and the design of a sprinkler system for uniform wetting.		

393 471

FOREWORD

Occasionally the engineer or analyst is confronted with the problem of dealing with a collection of moving particles. Fragments from exploding bombs, water from a sprinkling system, clouds of meteoroids in the vicinity of the earth, photons from a distant star, cosmic rays interacting with the magnetic field of the earth, all have a common thread in theoretical mechanics and are connected together in this report. Not much of the material is new, but the collection, simplification and unification of work from several specialized fields seemed worthwhile.

Accession For	
NTIS GRA&I	<input checked="" type="checkbox"/>
DDC TAB	<input type="checkbox"/>
Unannounced	<input type="checkbox"/>
Justification	
By _____	
Distribution/	
Availability Codes	
Dist	Avail and/or special
A	

TABLE OF CONTENTS

	Page
LIST OF ILLUSTRATIONS	7
1. INTRODUCTION	9
2. COORDINATE TRANSFORMATIONS FOR BASIC PHYSICAL QUANTITIES	13
3. TECHNIQUES FOR DEALING WITH MONODIRECTIONAL FLOWS	20
4. UNIFORM FORCE FIELDS	25
5. CENTRAL FORCE FIELDS AND ISOTROPIC DISTRIBUTIONS	29
6. MONOENERGETIC MONODIRECTIONAL FLOWS PAST A GRAVITATIONAL CENTER	38
7. FOCUSING OF PHOTONS BY A SCHWARZSCHILD FIELD	44
REFERENCES	57
APPENDIX 1	59
APPENDIX 2	61
DISTRIBUTION LIST	65

LIST OF ILLUSTRATIONS

Figure	Page
1. Relationship of velocity vectors in two coordinate systems, one of which moves with velocity \bar{V} along the Z axis of the other. The axes coincide at $t=0$	15
2. Some special functions. The derivative of function 1 is function 2 etc. Function 3 is the Dirac δ function. Functions 3 and 4 are shown as being finite for graphical purposes, but actually extend infinitely far	18
3. A depiction of monodirectional flow from a point source located at the point P. The areas dA include the trajectories of particles emitted into the solid angle $\sin\alpha \, d\alpha \, d\beta$	22
4. A depiction of a parallel stream interacting with an attractive center. The variable "a" may be defined as the impact parameter	23
5. Coordinates for the sprinkler problem. A particle emitted with speed v in a direction defined by α and β will fall at a position defined by ρ and ϕ	28
6. Distribution of water over a horizontal plane from a sprinkler which sprays isotropically. Each wetted point receives water from two directions	30
7. The geometry of grazing orbits. The conservation of angular momentum for a trajectory which grazes the earth requires that $r \, v(r) \, \sin\theta_m = R \, V(R)$	33
8. A plot of meteoroid number density versus distance from the earth measured in earth radii. At infinity the distribution is isotropic, uniform, and monoenergetic with speed U measured in units of escape velocity. The density at infinity is unity	35
9. A plot of meteoroid flux versus distance in earth radii for a distribution which at infinity is isotropic, monoenergetic with speed U and spatially uniform. U is measured in units of the escape velocity and the flux at infinity is unity	36

LIST OF ILLUSTRATIONS (CONT'D)

Figure	Page
10. Flow of a parallel stream of meteoroids from left to right past the earth. Points (1) shielded by the earth will see no meteoroids. Some points (2) will receive from one direction, and other (3) will receive from two directions. Points along the symmetry axis (4) will receive from all directions lying on the cone defined by the angle δ	40
11. Two trajectories which intersect at r and θ . The values for a_+ and a_- are obtained from Eq 6.10	43
12. An isoflux plot for a parallel stream of meteoroids moving by the earth at half the escape velocity ($U = 1/2$). The dotted lines are grazing orbits, which demarcate the region A receiving no flux, the region B receiving flux in one direction, and the region C receiving flux in two directions. Intensities are calculated by assuming unit flux at infinity	45
13. An isoflux plot for $U = 1$. For an explanation of the symbols, see Figure 12	46
14. An isoflux plot for $U = 2$. For an explanation of the symbols, see Figure 12	47
15. The lense effect associated with gravitational fields. The observer at (2) sees light from a distant star at (1) focused by a nearer star at (3) so that the star at (1) appears magnified and distorted. The angles are greatly exaggerated. The rays arriving at (2) from sources at (1) and (3) have an apparent angular separation δ	49
16. Description of the stellar disc in terms of angular displacements. The relationships of Eqs 7.23 and 7.24 are easily obtained by noting that $\theta_0 = \theta \cos \phi + \theta_1 \cos \phi_1$ and that $\theta \sin \phi = \phi_1 \sin \phi_1$. These two equations can be solved for θ_1 and ϕ_1	53
17. A depiction of what an observer sees as two stars move out of line. The vertical positions of the circles show the apparent angular separation of the three images and the sizes show the relative brightness. The nearer star is assumed to be on the horizontal zero line. It is clear that, although three images are theoretically possible, the third image is usually very dim. Thus optical binaries will look like optical binaries except in unusual circumstances	55

1. INTRODUCTION

Imagine a swarm of independent particles moving in space with the i th particle having a location defined by the position vector \bar{r}_i and a velocity \bar{v}_i . A unit volume with its center located by the position vector \bar{r} will contain $N(\bar{r}, t)$ particles at time t . The number $N(\bar{r}, t)$, called the particle density, may fluctuate in time and may be viewed as a probability density function as is common in statistical or quantum mechanics. The expression,

$$d N(\bar{r}, t) = N(\bar{r}, t) d\tau, \quad 1.1$$

may be defined as the number of particles expected in an element of volume $d\tau$. In an analogous manner, a swarm of particles can be described by a density function $N(\bar{r}, \bar{p}, t)$ in the six dimensional space of position vector \bar{r} and momentum vector \bar{p} such that the expression,

$$d N(\bar{r}, \bar{p}, t) = N(\bar{r}, \bar{p}, t) dx dy dz dp_x dp_y dp_z, \quad 1.2$$

is the probable number of particles contained at time t in the element of volume $dx dy dz dp_x dp_y dp_z$. By definition the expression,

$$N(\bar{r}, t) \equiv \iiint N(\bar{r}, \bar{p}, t) dp_x dp_y dp_z, \quad 1.3$$

defines the density of particles in the three-space defined by the coordinates x , y and z .

If the individual particles are moving in a force field such that a Hamiltonian H can be written for each of them, a Hamiltonian for the swarm can be written in terms of $N(\bar{r}, \bar{p}, t)$ and the variables \bar{r} and \bar{p} such that

$$\partial H / \partial x_i = -\dot{p}_i \equiv dp_i / dt \quad 1.4$$

and

$$\partial H / \partial p_i = \dot{x}_i \equiv dx_i / dt \quad 1.5$$

where the x_i are the position coordinates x , y and z and the p_i are the momenta associated with them. An arbitrary volume in the six dimensional space of \bar{r} and \bar{p} can be defined by particles on its surface as

$$V = \iiint \iiint \iiint dx_1 dx_2 dx_3 dp_1 dp_2 dp_3 \equiv \iiint \iiint \iiint d\tau \quad 1.6$$

so that from the divergence theorem,

$$\partial V / \partial t = \iiiii \bar{\nabla} \cdot \bar{v} d\tau, \quad 1.7$$

where $\bar{\nabla} \cdot \bar{v}$ is defined in the six space of \bar{r} and \bar{p} by the Einstein summation convention as

$$\bar{\nabla} \cdot \bar{v} d\tau = [\partial \dot{x}_i / \partial x_i + \partial \dot{p}_i / \partial p_i] d\tau \quad 1.8$$

Because of Eqs 1.4 and 1.5, Eq 1.8 becomes

$$\bar{\nabla} \cdot \bar{v} d\tau = \left[\frac{\partial^2 H}{\partial x_i \partial p_i} - \frac{\partial^2 H}{\partial p_i \partial x_i} \right] d\tau = 0 \cdot d\tau. \quad 1.9$$

Thus,

$$dV/dt = 0$$

for the volume defined in 6-space by a surface of moving particles. In particular, the elemental volume $d\tau$, associated with a particular particle as it moves in the space of \bar{r} and \bar{v} , is a constant of the motion. Thus, a collection of particles contained in an element of volume $d\tau$ may be defined at points 1 and 2 as

$$N(\bar{r}_1, \bar{p}_1, t_1) d\tau_1 = N(\bar{r}_2, \bar{p}_2, t_2) d\tau_2. \quad 1.10$$

Since $d\tau_1$ and $d\tau_2$ are equal,

$$N(\bar{r}_1, \bar{p}_1, t_1) = N(\bar{r}_2, \bar{p}_2, t_2), \quad 1.11$$

and $N(\bar{r}, \bar{p}, t)$ is also seen to be a constant along a particle trajectory in the space of \bar{r} and \bar{p} . This particular form of the Liouville theorem has proved useful in the treatment of meteoroid distributions and collisionless plasmas interacting with the magnetic field of the earth. These particular applications will be discussed more in detail later.

A detector will be defined as any surface sensitive to particle impacts. For a planar surface with a normal \hat{n} , the rate of impact $\phi(\bar{r}, \hat{n})$ from one side is given by the integral,

$$\phi(\bar{r}, \hat{n}) = \iiiii N(\bar{r}, \bar{v}) \bar{v} \cdot \hat{n} d\bar{v} dS, \quad 1.12$$

where $N(\bar{r}, \bar{v})$ represents the distribution of number with respect to position vector \bar{r} and velocity \bar{v} , $d\bar{v}$ is the element of volume in velocity space, and dS is an element of area. If the area is small and equal to A , Eq 1.12 can be written as

$$\phi(\bar{r}, \hat{n}) = A \int N(\bar{r}, \bar{v}) \bar{v} \cdot \hat{n} d\bar{v}. \quad 1.13$$

The simplest example of particle flow is that of a uniform monoenergetic monodirectional stream of particles with density N and velocity \bar{V} . In this case, Eq 1.13 becomes $\phi(\bar{r}, \hat{n}) = N\bar{V} \cdot \hat{n}A = JA \cos\theta$

where

$$J \equiv Nv \quad 1.14$$

and

$$\cos\theta \equiv \bar{v} \cdot \hat{n}/v. \quad 1.15$$

For a uniform monoenergetic isotropic distribution of speed v ,

$$N(\bar{r}, \bar{v}) = N/4\pi$$

$$\bar{v} \cdot \hat{n} \equiv v\cos\theta$$

and for a planar detector of unit area,

$$\phi(\bar{r}, \hat{n}) = (N/4\pi) \int_{\theta=0}^{\theta=\pi/2} \int_{\phi=0}^{\phi=2\pi} v\cos\theta \sin\theta d\theta d\phi = Nv/2. \quad 1.16$$

It is common in particle detection to define an isotropic spherical detector which presents unit area to all directions. The count rate ϕ for such a detector is given by

$$\phi = \iiint N(\bar{r}, \bar{v}) v d\bar{v}. \quad 1.17$$

For the uniform monoenergetic monodirectional stream above,

$$\phi = Nv \quad 1.18$$

and for the isotropic distribution,

$$\phi = Nv. \quad 1.19$$

The measurement ϕ described by Eq 1.17 is usually called the particle flux and is measured in $p/m^2 \text{ sec}$. In a unit volume, if there are N_i particles with speed V_i , ϕ can be defined as

$$\phi = \sum_i N_i v_i = Nv \quad 1.20$$

where

$$N = \sum_i N_i \quad 1.21$$

and

$$v \equiv \sum_i N_i v_i / \sum_i N_i. \quad 1.22$$

Occasionally we need to compute the rate $\phi(\bar{r}, \hat{n})$ at which particles fall on an element of surface $\hat{n} ds$ located at \bar{r} when the particle source is located at the coordinate origin and has an emission described by $S(\bar{V})$ p/ster sec. In this case

$$\phi(\bar{r}, \hat{n}) = s(\bar{V}) ds (\hat{r} \cdot \hat{n}) / r^2. \quad 1.23$$

The expression $ds \hat{r} \cdot \hat{n} / r^2$ is defined as the solid angle subtended by the surface ds as measured from the source located at the origin.

A particularly interesting and useful interpretation of the Liouville theorem has been applied to the motion of charged particles in electromagnetic fields, a subject of interest to geophysicists studying the population of particles captured in the magnetic field of the earth and to particle physicists trying to promote thermonuclear reactions among particles contained in a magnetic bottle. Suppose that a particle trajectory is defined by $\bar{r}(t)$ and that its velocity is therefore $\bar{v}(\bar{r}, t) \equiv d\bar{r}/dt$. Suppose that, at some point \bar{r} , on the particle trajectory, a directional counter sensitive to an element of solid angle dw is pointed along the particle trajectory so that its counting rate $C(\bar{r}_1)$ is given by

$$C(\bar{r}_1, \bar{v}_1) = \iiint N(\bar{r}_1, \bar{v}) v dv dw = dw \int N(\bar{r}_1, \bar{v}_1) v dv \quad 1.24$$

Since a constant magnetic field does not change the speed of a particle, at some other point \bar{r}_2 on the particle trajectory.

$$C(\bar{r}_2, \bar{v}_2) = C(\bar{r}_1, \bar{v}_1), \quad 1.25$$

where it is understood that both counting rates are obtained by pointing the directional detector along the trajectory of a particular particle. Eq 1.25 is just an experimental way of expressing the Liouville theorem for a limited application. The integral in Eq 1.24 gives the counting rate for a directional detector but also defines a small element of volume in \bar{r} - \bar{p} space. When this same element of volume in phase space is sampled at another point (or an equivalent volume in a time independent system of particles), it must contain the same number of particles and

result in the same counting rate.

When the first American satellites were placed in orbit about the earth, they carried directional detectors for charged particles. It was possible by means of Eq 1.25 to infer the particle density for the entire region around the earth by making measurements only in the equatorial plane.

2. COORDINATE TRANSFORMATIONS FOR BASIC PHYSICAL QUANTITIES

Occasionally it is easier to perform an analysis in one coordinate system and to transform to another for which an answer is needed than to perform an analysis in the final coordinate system. Also, measurements may be made in the wrong coordinate system for easy application. If a particle has a velocity \bar{v} in the primary reference system and a velocity \bar{v}' in another system moving at a velocity \bar{V} relative to the primary system, the velocities are related by the classical addition law,

$$\bar{v} = \bar{V} + \bar{v}', \quad 2.1$$

and the position vectors are related by the equation,

$$\bar{r} = \bar{R} + \bar{r}', \quad 2.2$$

where \bar{R} connects the coordinate origins.

If a collection of particles are observed in each system and the total number of particles N in an arbitrary volume is given by the equations

$$N = \iiint \iiint N(\bar{r}, \bar{v}, t) d\tau = \iiint \iiint N'(\bar{r}', \bar{v}', t) d\tau', \quad 2.3$$

the relationship of the density functions is given by

$$N(\bar{r}, \bar{v}, t) d\tau = N[\bar{r}(\bar{r}'), \bar{v}(\bar{v}')] D\left(\frac{\bar{r}, \bar{v}}{\bar{r}', \bar{v}'}\right) d\tau' \quad 2.4$$

so that

$$N'(\bar{r}', \bar{v}') = N[\bar{r}(\bar{r}'), \bar{v}(\bar{v}')] D\left(\frac{\bar{r}, \bar{v}}{\bar{r}', \bar{v}'}\right). \quad 2.5$$

The symbol D is the Jacobian associated with the transformation of coordinate differentials.

As an example, suppose that the distribution in the first system is isotropic and that the distribution in a system moving with speed \bar{V} along the zz' axis is desired. We will define

$$d\tau = dx dy dz V^2 \sin\theta dv d\theta d\phi \quad 2.6$$

in the first system. Note that cartesian coordinates are used in \bar{r} space and spherical coordinates are used in \bar{v} space. If the coordinate origins and coordinate axes coincide in \bar{r} space, from Eq 2.2

$$\bar{r} = \bar{r}' \quad 2.7$$

and

$$dx dy dz = dx' dy' dz'. \quad 2.8$$

From Eq 2.1

$$\bar{v} = \bar{V} + \bar{v}' \quad 2.9$$

and

$$v^2 = V^2 + (v')^2 + 2Vv' \cos\epsilon. \quad 2.10$$

If the coordinate areas are chosen so that \bar{V} coincides with the z and z' axes, ϵ becomes θ' in the $r'\theta'\phi'$ system, as shown in Figure 1. It is evident from Figure 1 that

$$v^2 = V^2 + (v')^2 + 2 Vv' \cos\theta' \quad 2.11$$

$$V' \sin\theta' = v \sin\theta \quad 2.12$$

$$\phi' = \phi \quad 2.13$$

so that the Jacobian can be written after some algebra as

$$D\left(\frac{\bar{r}, \bar{v}}{\bar{r}', \bar{v}'}\right) = \begin{vmatrix} \frac{\partial v}{\partial v'} & \frac{\partial \theta}{\partial v'} \\ \frac{\partial v}{\partial \theta'} & \frac{\partial \theta}{\partial \theta'} \end{vmatrix} = v'/v. \quad 2.14$$

Thus

$$N'(\bar{r}, v') = N[\bar{r}(\bar{r}'), \bar{v}(\bar{v}')] v'/v. \quad 2.15$$

In the limit as v' becomes small, \bar{v} and \bar{V} become the same, as seen from Figure 1 or Eq 2.11, and the distribution becomes monoenergetic and monodirectional with velocity \bar{V} . If \bar{V} becomes small, v and v' become the same and the distributions become equal. For the particular case of a uniform isotropic distribution such that

$$N(\bar{r}, \bar{v}) = A, \quad v_1 < v < v_2, \quad 2.16$$

the particles are contained in velocity space between two spheres of

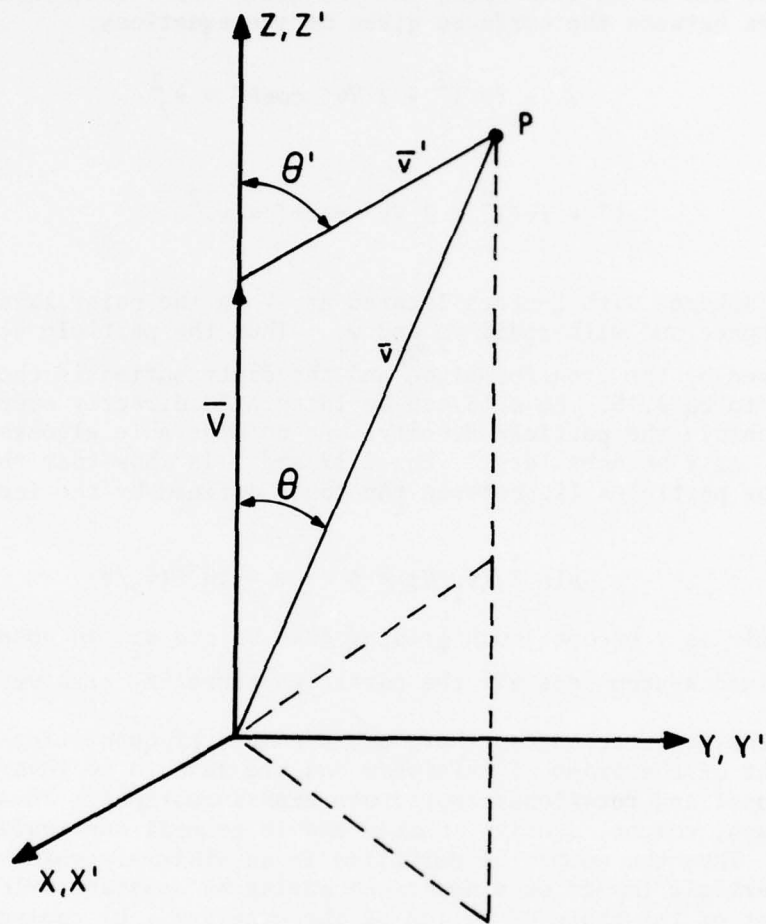


Figure 1. Relationship of velocity vectors in two coordinate systems, one of which moves with velocity \bar{V} along the Z axis of the other. The axes coincide at $t=0$.

radius v_1 and v_2 . The density, $4\pi A(v_2^3 - v_1^3)/3$, is just the volume between these two spheres multiplied by A . In the primed coordinate system, the use of Eq 2.10 shows the particles to be contained in the volumes between the surfaces given by the equations,

$$V^2 + (v')^2 + 2 Vv' \cos\theta' = v_2^2 \quad 2.17$$

and

$$V^2 + (v')^2 + 2 Vv' \cos\theta' = v_1^2. \quad 2.18$$

These are spheres with centers located at $-V$ on the polar axis in velocity space and with radii v_2 and v_1 . Thus the particle density is conserved by the transformation and the distribution is changed according to Eq 2.15. Eq 2.15 can be integrated directly over velocity space to obtain the particle density, but considerable algebra is involved. As V becomes large, Eqs 2.17 and 2.18 show that the velocity vectors for particles lie between the cones defined by the inequalities,

$$\pi - \sin^{-1}(v_1/V) \leq \theta' \leq \pi - \sin^{-1}(v_2/V). \quad 2.19$$

In the limit as V becomes much greater than v_1 and v_2 , an observer in the primed system sees all the particles traveling with velocity $-\bar{V}$.

In classical mechanics, there are a number of quantities which are independent of the frame of reference and are said to be invariant to translational and rotational coordinate transformations. These include mass, volume, density, number and in general any scalar quantity. Thus the number of particles in an arbitrary volume or the rate of particle impact on a detector moving at constant velocity are independent of the state of motion of the observer. Of course, if the state of motion of the detector is changed, it sees a different particle distribution in velocity space as discussed above. In general it is easier to compute impacts on a detector at rest than it is to compute impacts when both detector and particles are moving. Eq 2.15 permits the computation of the particle distribution in the coordinate system for which the detector is at rest. In this coordinate system, the definitions of Table 1 are made.

Table 1. Definition of Various Physical Quantities in Terms of the Density Function in Six-Space

1. Total number of particles	$\iiint\iiint\iiint N(\bar{r}, \bar{v}) d\bar{r}d\bar{v} \equiv N$
2. Density of particles (Number/m ³)	$\iiint N(\bar{r}, \bar{v}) d\bar{v} \equiv N(\bar{r})$
3. Counting rate by a unit isotropic detector	$\iiint N(\bar{r}, \bar{v}) v d\bar{v} \equiv \phi(\bar{r})$
4. Counting rate by a unit Surface detector with normal \hat{n} .	$\iiint N(\bar{r}, \bar{v}) \bar{v} \cdot \hat{n} d\bar{v} = \phi(\bar{r}, \hat{n})$

Because of its association with idealized particle distributions with respect to \bar{r} and \bar{v} , it is useful to enumerate some of the properties of the Dirac δ function and to use it to represent several distributions of common interest. A graphical depiction of the δ function and others related to it are shown in Figure 2. By definition, if the range of integration includes the origin,

$$\int_{x=a}^{x=b} f(x) \delta(x) dx = f(0). \quad 2.20$$

It follows that

$$\int_{x=a}^{x=b} \delta(x) dx = 1 \quad 2.21$$

If $x = y - a$ 2.22

so that $y = x + a$ 2.23

then

$$\int_{y=b}^{y=c} f(y) \delta(y-a) dy = \int_{x=b-a}^{x=c-a} f(x+a) \delta(x) dx = f(a) \quad 2.24$$

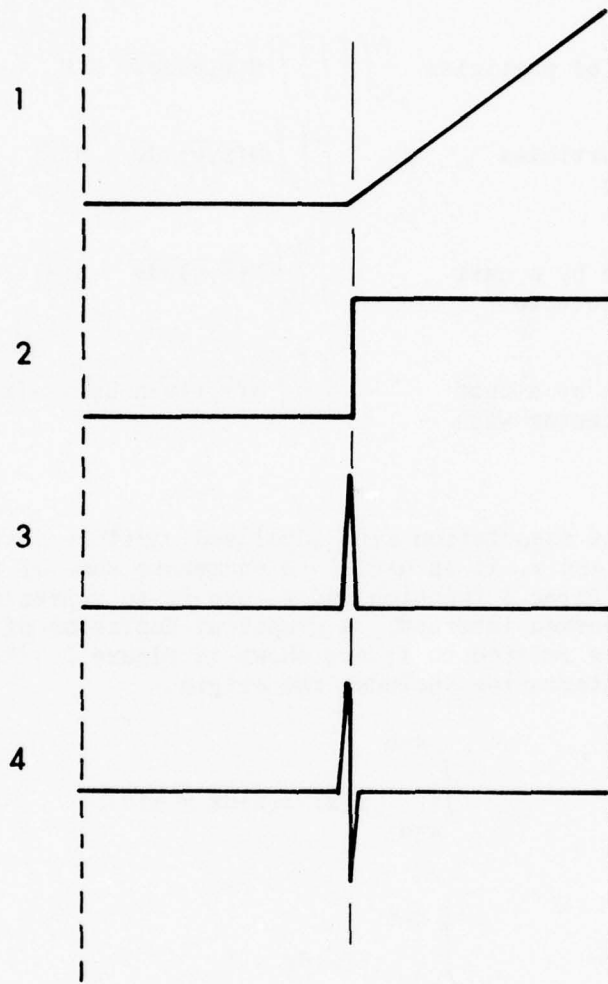


Figure 2. Some special functions. The derivative of function 1 is function 2 etc. Function 3 is the Dirac δ function. Functions 3 and 4 are shown as being finite for graphical purposes, but actually extend infinitely far.

Thus, since the variable of integration is immaterial,

$$\int_{x=b}^{x=c} f(x) \delta(x-a) dx = f(a). \quad 2.25$$

Suppose that

$$y = F(x) \quad 2.26$$

and

$$x = G(y). \quad 2.27$$

Then

$$\int_{x=b}^{x=c} \delta[x-a] dx = \int_{y=B}^{y=C} \delta[G(y) - G(A)] (dG/dy) dy = 1. \quad 2.28$$

where $y=A$ when $x=a$.

Thus

$$\delta(y-A) dy = \delta[G(y) - a] (dG/dy) dy \quad 2.29$$

or

$$\delta(y-A) = \delta[G(y) - a] dG/dy. \quad 2.30$$

As an example, suppose that

$$y = x^2 \quad 2.31$$

and

$$x = y^{1/2} \quad 2.32$$

and that we wish to evaluate the integral

$$\int x^3 \delta(x-a) dx = a^3. \quad 2.33$$

With a change in variables according to Eqs 2.31 and 2.32, the integral becomes

$$\int y^{3/2} \delta[y^{1/2}-a] [(1/2)y^{-1/2}] dy. \quad 2.34$$

By using Eq 2.30 with the definition $A = a^2$, this becomes

$$\int y^{3/2} \delta(y-A) dy = (A)^{3/2} = a^3. \quad 2.35$$

The δ function concept can be extended with care to more than one dimension. For example, the definition,

$$\delta(\bar{r}) \equiv \delta(x) \delta(y) \delta(z), \quad 2.36$$

permits the expressions

$$\iiint F(\bar{r}) \delta(\bar{r}) d\tau = F(0), \quad 2.37$$

and

$$\iiint F(\bar{r}) \delta(\bar{r}-\bar{r}_0) d\tau = F(\bar{r}_0). \quad 2.38$$

It should be noted that δr defined in spherical coordinates is not equivalent to $\delta(x) \delta(y) \delta(z)$ although there are strong similarities. As a rule, it is easier to deal with continuous rather than discrete distributions because of the difficulty of mapping the δ function from one coordinate system to another, especially if there are several variables.

3. TECHNIQUES FOR DEALING WITH MONODIRECTIONAL FLOWS

In dealing with particle fields which are locally monodirectional, i.e. all particles in the neighborhood of a point in r space are traveling in the same direction, the Liouville theorem and the Dirac delta function are not particularly useful. The photons from a distant star, a collection of meteoroids moving in a loosely connected cloud through the solar system, or the droplets from a sprinkler system are examples of locally monodirectional flows. Suppose as shown in Figure 3 that a point source emits particles at a constant rate $S(\alpha, \beta)$, measured in particles/(steradian second), into the element of solid angle $\sin\alpha d\alpha d\beta$. If the flow is time independent, at any point on a particle trajectory we must have

$$s(\alpha, \beta) \sin\alpha d\alpha d\beta = J dA \quad 3.1$$

where J is the current density, measured in particles/m²sec, and dA is an element of area normal to the particle trajectories. Solving for J we find

$$J = S(\alpha, \beta) \sin\alpha d\alpha d\beta / dA. \quad 3.2$$

The central problem in monodirectional flows is to find the magnitude and direction of the current J in a convenient coordinate system.

In Figure 3, three coordinate systems may be visualized. The source location at P may be viewed as a coordinate origin from which it is convenient to describe particle emission in terms of $S(\alpha, \beta)$. An observer at point 0 may wish to measure $J(\vec{r})$ in terms of convenient spherical or Cartesian systems with origin at point 0. For convenience in calculating the vector current density \vec{J} , it would be convenient to have a coordinate system based on the normal and tangent unit vectors of particle trajectories.

Instead of the point source of Figure 3, a parallel stream passing an attractive center is shown in Figure 4. Following the same line of reasoning as before,

$$J(\vec{r}) = J(\rho, \delta) a \, da \, d\delta/dA \quad 3.3$$

where $J(\rho, \delta)$ is the current density distribution at a point distant from the attractive center and $J(\vec{r})$ is the perturbed current density near it.

In general it is easy to establish an element of area dA' which contains the point located by \vec{r} , but it must be projected onto the plane normal to the trajectory such that

$$dA = dA' \cos \epsilon, \quad 3.4$$

where ϵ is the angle between the normals of dA and dA' . In spherical coordinates, for example, any one of three elemental areas can be chosen, videlicet,

$$dA' = r \, dr \, d\theta \, \hat{\phi}, \quad 3.5$$

or

$$dA' = r \sin \theta \, dr \, d\phi \, \hat{\theta}, \quad 3.6$$

or

$$dA' = r^2 \sin \theta \, d\theta \, d\phi \, \hat{r}, \quad 3.7$$

where \hat{r} , $\hat{\theta}$ and $\hat{\phi}$ are the appropriate unit vectors defined by the spherical coordinate system to be normal to the elemental areas.

The trajectory or orbit of a particle may be expressed, in terms of the variables defined by Figure 3, as the intersection of two surfaces,

$$F(r, \theta, \phi, \alpha) = 0 \quad 3.8$$

and

$$G(r, \theta, \phi, \beta) = 0. \quad 3.9$$

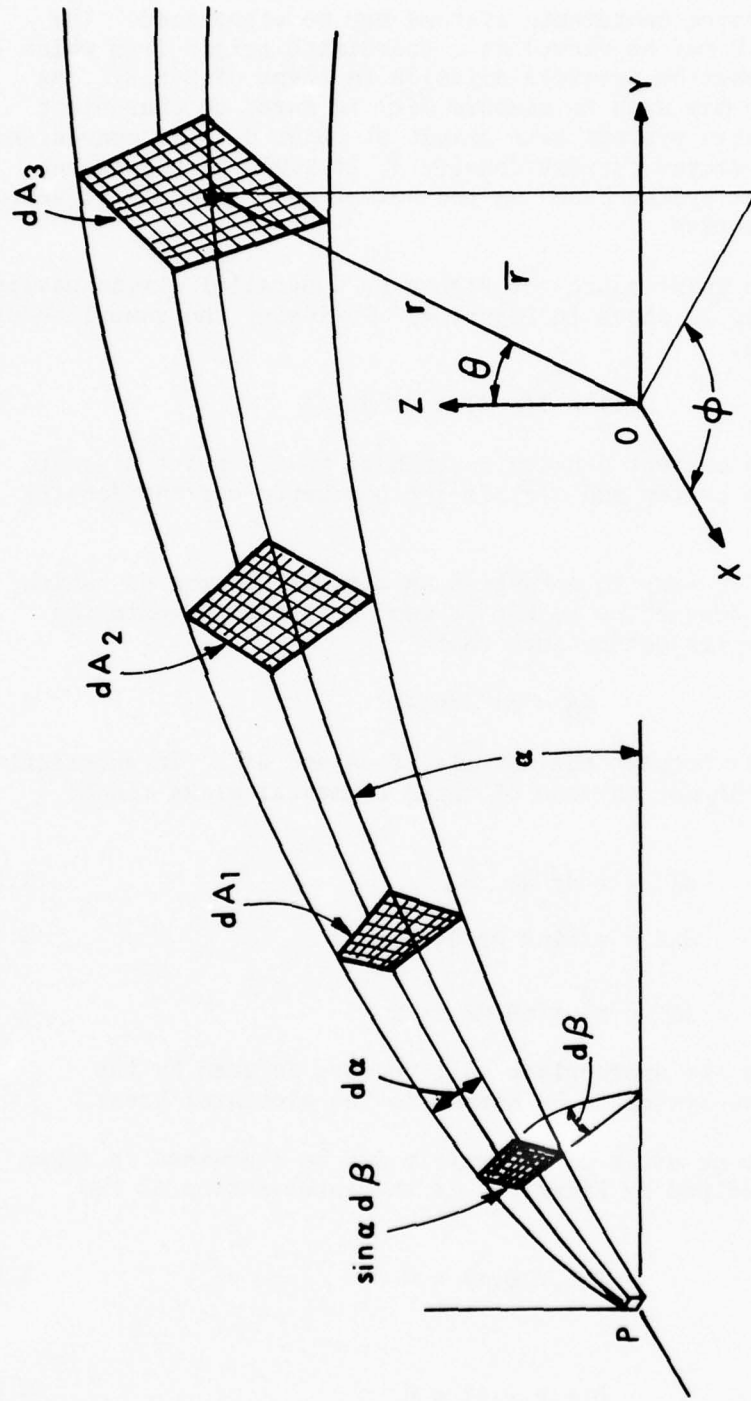


Figure 3. A depiction of monodirectional flow from a point source located at the point P . The areas dA include the trajectories of particles emitted into the solid angle $\sin\alpha d\alpha d\beta$.

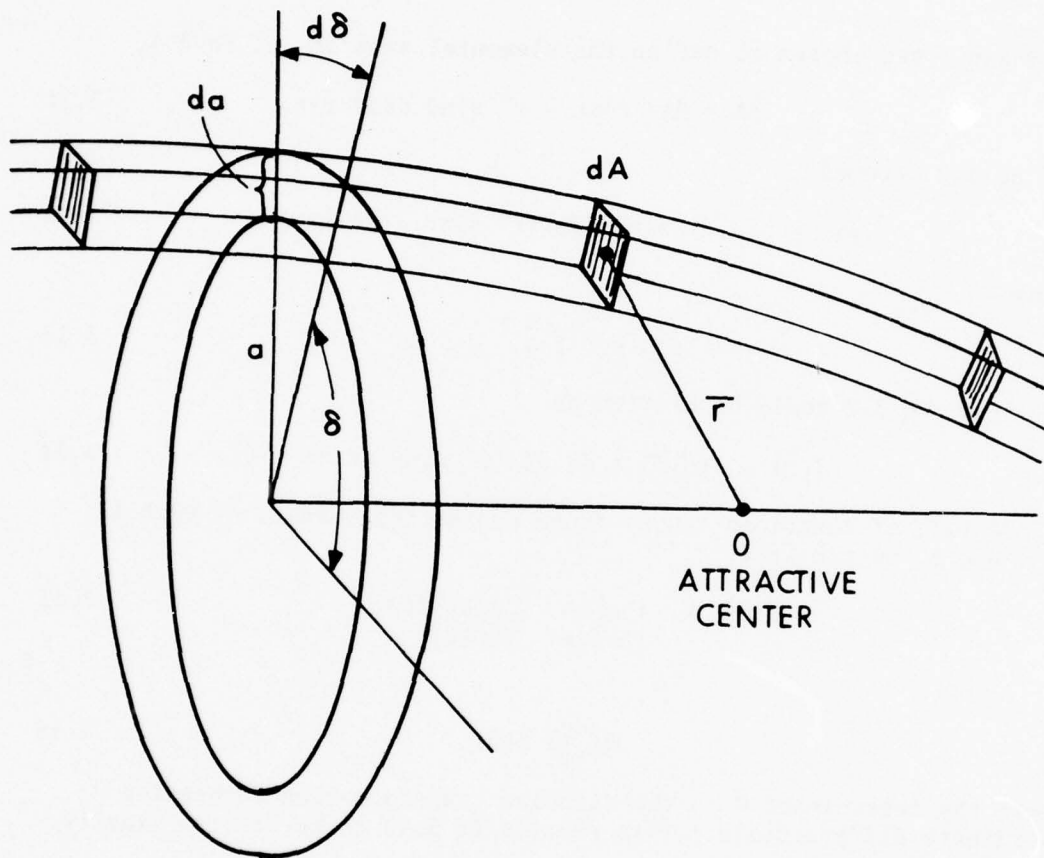


Figure 4. A depiction of a parallel stream interacting with an attractive center. The variable "a" may be defined as the impact parameter.

A third coordinate surface may be defined by the distance the particle has traveled from the source. Since the functions $\bar{\nabla}F$ and $\bar{\nabla}G$ are normal to the trajectory, they can be used to define a unit vector \hat{t} which is tangent to the trajectory by the equation,

$$\hat{t} = (\bar{\nabla}F \times \bar{\nabla}G) / |\bar{\nabla}F \times \bar{\nabla}G|. \quad 3.10$$

If θ and ϕ are chosen to define the elemental area dA' of Eq 3.4,

$$dA = dA' \cos \epsilon = r^2 \sin \theta \, d\theta \, d\phi \, \hat{r} \cdot \hat{t}, \quad 3.11$$

and Eq 3.2 becomes

$$J(\bar{r}) = s(\alpha, \beta) \sin \alpha \, d\alpha \, d\beta / [r^2 \sin \theta \, d\theta \, d\phi \, \hat{r} \cdot \hat{t}], \quad 3.12$$

where

$$\cos \epsilon \equiv \hat{r} \cdot \hat{t}. \quad 3.13$$

Likewise, Eq 3.3 could be written as

$$J(\bar{r}) = J(\rho, \delta) \, a \, da \, d\delta / [r^2 \sin \theta \, d\theta \, d\phi \, \hat{r} \cdot \hat{t}]. \quad 3.14$$

In general, if equations can be found connecting α and β of Eq 3.12 to θ and ϕ , we can write

$$d\alpha \, d\beta = \begin{vmatrix} \partial\alpha/\partial\theta & \partial\beta/\partial\theta \\ \partial\alpha/\partial\phi & \partial\beta/\partial\phi \end{vmatrix} d\theta \, d\phi \quad 3.15$$

$$\equiv D\left(\frac{\alpha\beta}{\theta\phi}\right) d\theta \, d\phi \quad 3.16$$

where the determinant D is the Jacobian transformation connecting coordinate differentials. This permits Eq 3.12 to be written finally as

$$J(\bar{r}) = s(\alpha, \beta) \sin \alpha \, D\left(\frac{\alpha\beta}{\theta\phi}\right) / [r^2 \sin \theta \, \hat{r} \cdot \hat{t}]. \quad 3.17$$

Eq 3.17 contains formally the magnitude $J(\bar{r})$ and direction \hat{t} of the vector current density at an arbitrary point in space with \hat{t} given by Eq 3.10.

If particles are neither created or destroyed during steady-state flow, the continuity equation may be written as

$$\bar{v} \cdot \bar{J} + \frac{\partial N}{\partial t} = 0 \quad 3.18$$

and since by definition of steady-state flow

$$\partial N / \partial t = 0 \quad 3.19$$

we must have

$$\bar{v} \cdot \bar{J} = 0 \quad 3.20$$

or divergenceless flow. The preceding discussion of course is based on the assumption of divergenceless flow and a corollary that the flow contained in a bundle of streamlines is the same across any area defined by the streamlines and normal to them. Thus

$$J(\bar{r}_1)A(\bar{r}_1) = J(\bar{r}_2)A(\bar{r}_2) \quad 3.21$$

or

$$N(\bar{r}_1)V(\bar{r}_1)A(\bar{r}_1) = N(\bar{r}_2)V(\bar{r}_2)A(\bar{r}_2) \quad 3.22$$

for any two points on a particle trajectory.

4. UNIFORM FORCE FIELDS

To illustrate the usefulness of the techniques developed in the foregoing pages, two standard problems, dealing with idealized waterfalls and sprinklers, will be examined from several viewpoints.

We will assume in the waterfall problem that we have a vertical fall, in a uniform gravitational field, of particles which do not interfere with each other and that the flow is constant in time. If Z is the distance measured downward from the coordinate origin, Eq 3.22 yields the solution,

$$N(Z)v(Z) = N(0)v(0) \quad 4.1$$

where the conservation of energy equation,

$$v^2(Z)/2 + gZ = v^2(0)/2, \quad 4.2$$

yields $v(Z)$ as

$$v(Z) = [-2gZ + v^2(0)]^{1/2}. \quad 4.3$$

In these equations $v(0)$ is the speed when Z is zero and g is the gravitational acceleration.

The waterfall problem could be approached more generally by assuming a distribution of velocities given by

$$N(0, v) = K \quad , \quad v_1 < v < v_2. \quad 4.4$$

The Liouville theorem permits $N(Z, v)$ to be written as

$$N(Z, v) = K \quad ; \quad v_1(Z) < v < v_2(Z), \quad 4.5$$

where from Eq 4.3,

$$v_1(Z) = [v_1^2 - 2gZ]^{1/2} \quad 4.6$$

and

$$v_2(Z) = [v_2^2 - 2gZ]^{1/2} \quad 4.7$$

By definition,

$$\begin{aligned} N(Z) &= \int_{v_1(Z)}^{v_2(Z)} N(Z, v) dv \\ &= K [v_2(Z) - v_1(Z)]. \end{aligned} \quad 4.8$$

In the limit as v_1 approaches v_2 , v_1 and v_2 can be replaced by $v(0)$ and $v_2 - v_1$ by $\Delta v(0)$. From Eq 4.8

$$N(Z) = K \Delta v(Z) \quad 4.9$$

and from Eqs 4.6 and 4.7

$$\Delta v(Z) = v(0) \Delta v(0) / [v^2(0) - 2gZ]^{1/2} \quad 4.10$$

so that

$$N(Z) = K v(0) \Delta v(0) / [v(0)^2 - 2gZ]^{1/2}. \quad 4.11$$

From Eqs 4.1 and 4.3

$$N(Z) = N_0 v(0) / [v(0)^2 - 2gZ]^{1/2} \quad 4.12$$

If $K v(0) \Delta v(0)$ is identified with $N(0)v(0)$, Eqs 4.11 and 4.12 are the same, thus demonstrating the value of the Liouville theorem.

In the more complex sprinkler problem, let us assume that a water sprinkler emits droplets according to the density function $S(v, \alpha, \beta)$. This means that the expression $S(v, \alpha, \beta) v^2 dv \sin\alpha d\alpha d\beta$ defines in velocity space the number of particles emitted each second having speeds between v and $v + dv$ and direction lying in the solid angle $\sin\alpha d\alpha d\beta$. The problem is to find the rate at which particles fall on an arbitrary unit area in the plane containing the sprinkler. The coordinates of the problem are defined in Figure 5. The choice of the coordinate system permits the equality of β and ϕ .

Starting with Newton's second law, the trajectory for a particle emitted with speed v in the direction defined by α and β is given by

$$\phi = \beta = \text{constant} \quad 4.13$$

$$\rho = v \sin\alpha t \quad 4.14$$

$$Z = v \cos\alpha t - gt^2/2 \quad 4.15$$

where t is the time elapsed after launch and g is the gravitational acceleration.

The particle hits the surface when Z equals zero so that

$$\rho = (2v^2/g) \sin\alpha \cos\alpha = (v^2/g) \sin 2\alpha \quad 4.16$$

If it is assumed that the emission at speed v in the solid angle $\sin\alpha d\alpha d\beta$ falls into the elemental area $\rho d\rho d\phi$ and it is recalled that ϕ and β are identical,

$$S(\alpha, \phi) \sin\alpha d\alpha d\phi = J \cos \epsilon \rho d\rho d\phi \quad 4.17$$

and

$$J \cos \epsilon = \frac{S(\alpha, \phi) \sin\alpha d\alpha}{\rho d\rho} \equiv J_Z \quad 4.18$$

From Eq 4.16,

$$\frac{d\rho}{d\alpha} = 2(v^2/g) \cos 2\alpha \quad 4.19$$

so that

$$\begin{aligned} J_Z &= \frac{S(\alpha, \phi) \sin\alpha}{2(v^4/g^2) \sin 2\alpha \cos 2\alpha} \quad 4.20 \\ &= \frac{S(\alpha, \phi) \sin\alpha}{(v^4/g^2) \sin 4\alpha} \end{aligned}$$

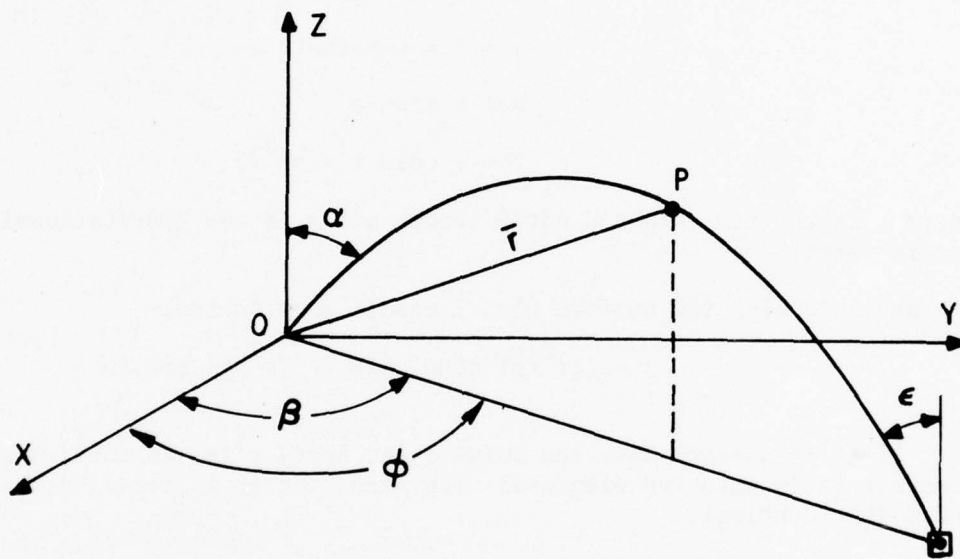


Figure 5. Coordinates for the sprinkler problem. A particle emitted with speed v in a direction defined by α and β will be at a position defined by ρ and ϕ .

where from Eq 4.16

$$\alpha = (1/2) \sin^{-1} (\rho g/v^2), \quad 0 \leq \alpha \leq \pi/2 \quad 4.21$$

For the particular case of the isotropic source,

$$S \equiv \dot{Q}/2\pi \quad 4.22$$

where \dot{Q} is the total water flow,

$$J_z = (\dot{Q}/2\pi) \sin \alpha / [(v^4/g^2) \sin 4\alpha]. \quad 4.23$$

For this particular case there is symmetry in the trajectory and \hat{t} is obtained by inspection to be given by equation,

$$\hat{t} = -\hat{k} \cos \alpha + \hat{i} \sin \alpha \cos \phi + \hat{j} \sin \alpha \sin \phi, \quad 4.24$$

which is just a reflection of the original direction of emission in the x y plane.

It should be noted that $d\rho/d\alpha$ changes sign when $\alpha = \pi/4$, the angle which gives maximum range. Thus each wetted area receives two flows, one for $0 \leq \alpha < \pi/4$ and one for $\pi/4 < \alpha \leq \pi/2$. These are plotted in Figure 6. If it is desired to produce a sprinkler which wets uniformly, Eq 4.23 tells us that we must have

$$S(\alpha, \phi) = k[(v^4/g^2) \sin 4\alpha] / \sin \alpha, \quad 4.25$$

where k is a constant of proportionality.

5. CENTRAL FORCE FIELDS AND ISOTROPIC DISTRIBUTIONS

When manned space flight was in its early stages there was a considerable interest in the distribution of meteoroids about the earth. If the meteoroid distribution about the earth were assumed to be isotropic in direction, a theoretical treatment by S. F. Singer¹ yielded the density of meteoroids as a function of velocity at infinity and distance from the earth. If the meteoroids were thought to consist of a locally monodirectional stream flowing by the earth, a theoretical treatment by R. D. Shelton² et al gave the density and flux distributions.

¹S. F. Singer, *Nature*, Oct 78, 1961, pp 321-323.

²R. D. Shelton, et al, *Astronomical Journal* 70 No. 2, Mar 1965, pp 166-170.

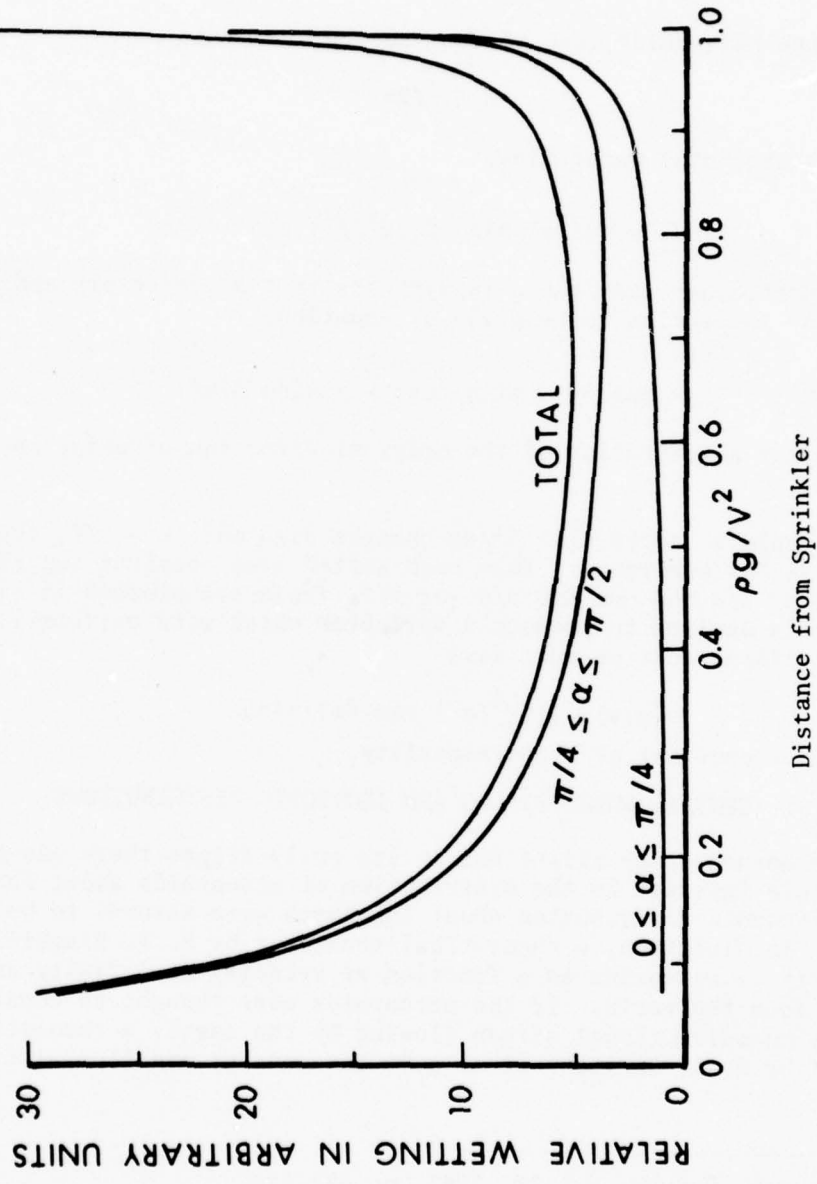


Figure 6. Distribution of water over a horizontal plane from a sprinkler which sprays isotropically. Each wetted point receives water from two directions.

The following discussion of isotropic meteoroid distributions differs slightly from that of Singer, but illustrates the use of techniques previously developed and obtains the same results. Let the meteoroid population far from the earth be given by

$$S(\bar{r}) = K = S(\infty) ; v_1 < v < v_2. \quad 5.1$$

The density at infinity is given by definition as,

$$N(\bar{r}) = \iiint K v^2 dv \sin\theta d\theta d\phi = (4\pi K/3)(v_2^3 - v_1^3) = N(\infty). \quad 5.2$$

The flux measured by an isotropic unit detector would be given as

$$\phi(\bar{r}) = \iiint K v^3 dv \sin\theta d\theta d\phi = \pi K(v_2^4 - v_1^4) = \phi(\infty). \quad 5.3$$

In the above formulae, v , θ and ϕ are coordinates in velocity space.

The conservation of energy for particles passing near the earth requires that

$$v_\infty^2 = v^2(\bar{r}) - 2GM/r, \quad 5.4$$

where v_∞ is the particle speed at infinity, $v(\bar{r})$ is the particle speed after it has moved to a location \bar{r} , G is the gravitational constant and M is the mass of the earth. The Liouville theorem and Eq 5.1 require that

$$S(\bar{r}) = K ; v_1(\bar{r}) \leq v \leq v_2(\bar{r}) \quad 5.5$$

where from Eqs 5.1 and 5.4

$$v_1(\bar{r}) = [v_1^2 + 2GM/r]^{1/2} \quad 5.6$$

and

$$v_2(\bar{r}) = [v_2^2 + 2GM/r]^{1/2}. \quad 5.7$$

Therefore

$$\begin{aligned}
 N(\bar{r}) &= \iiint K v^2 dv \sin\theta d\theta d\phi \\
 &= (4\pi K/3) \{ [v_2^2 + 2GM/r]^{3/2} - \\
 &\quad [v_1^2 + 2GM/r]^{3/2} \}
 \end{aligned} \tag{5.8}$$

and

$$\phi(\bar{r}) = \pi K \{ [v_2^2 + 2GM/r]^2 - [v_1^2 + 2GM/r]^2 \} \tag{5.9}$$

In the limit as v_1 and v_2 approach v_∞ (i.e., the distribution is monoenergetic and isotropic), and their difference becomes ΔV , Eqs 5.8 and 5.9 may be written as

$$N(\bar{r})/N(\infty) = v(\bar{r})/v_\infty \tag{5.10}$$

and

$$\phi(\bar{r})/\phi(\infty) = [v(\bar{r})/v_\infty]^2 \tag{5.11}$$

where

$$v(\bar{r}) = [v_\infty^2 + 2GM/r]^{1/2} \tag{5.12}$$

The meteoroid distribution is diminished near the earth because the earth stops the motion of meteoroids whose trajectories intersect it. By using the principle of conservation of angular momentum, as shown in Figure 7, we can write

$$R v(R) = r v(r) \sin\theta_m \tag{5.13}$$

so that

$$\sin\theta_m = R v(R)/r v(r). \tag{5.14}$$

The fractional solid angle f available at point P is given by

$$f = \frac{1}{4\pi} \int_{\phi=0}^{\phi=2\pi} \int_{\theta=0}^{\theta=\pi-\theta_m} \sin\theta d\theta d\phi. \tag{5.15}$$

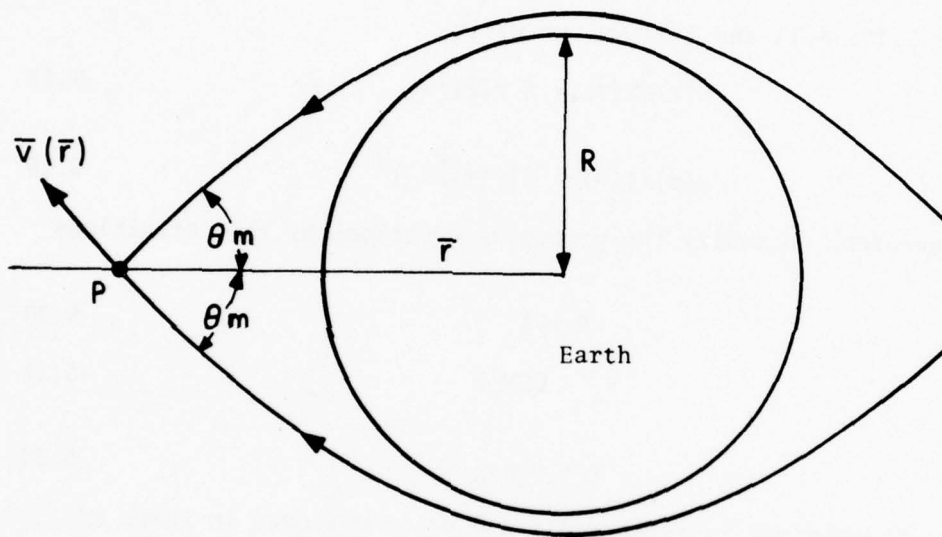


Figure 7. The geometry of grazing orbits. The conservation of angular momentum for a trajectory which grazes the earth requires that $r v(r) \sin\theta_m = R V(R)$.

From Eq 5.13

$$\cos \theta_m = [1 - \sin^2 \theta_m]^{1/2} = [1 - R^2 v^2(R) / r^2 v^2(r)]^{1/2} \quad 5.16$$

so that, using Eqs 5.4, 5.15 and 5.16,

$$f = 1/2 \{1 + [1 - (R/r)^2 (v_\infty^2 + 2GM/R) / (v_\infty^2 + 2GM/r)]^{1/2}\}. \quad 5.17$$

As expected, f goes to $1/2$ near the earth and to unity at large distances.

Using Eqs 5.10, 5.11 and 5.17 we can write

$$N(r)/N(\infty) = f v(r)/v_\infty \quad 5.18$$

$$\phi(r)/\phi(\infty) = f [v(r)/v_\infty]^2 \quad 5.19$$

It is convenient to modify the preceding equations by the definitions

$$R = 1 \quad 5.20$$

$$v_e \equiv 2GM/R \quad 5.21$$

and

$$v = v_\infty / v_e \quad 5.22$$

so that r is measured in earth radii and v_∞ is measured in terms of the escape velocity. Eq 5.4 now becomes

$$v^2(r) = v_\infty^2 + (2GM/R)(R/r) = v^2 + 1/r \quad 5.23$$

and Eqs 5.10 and 5.11 becomes

$$N(\bar{r})/N(\infty) = [1 + 1/(rV^2)]^{1/2} (1/2) \{1 + [1 - (1/r)^2 (V^2 + 1)/(V^2 + 1/r)]^{1/2}\} \quad 5.24$$

$$\phi(\bar{r})/\phi(\infty) = [1 + 1/(rV^2)] (1/2) \{1 + [1 - (1/r)^2 (V^2 + 1)/(V^2 + 1/r)]^{1/2}\} \quad 5.25$$

Note that, as r goes to infinity, these ratios go to unity as expected physically. As V becomes large and the earth has no influence, these ratios are diminished by the fraction of the total solid angle subtended by the earth at distance r , namely R^2/r^2 . Eq 5.23 is the same as Singer's Eq 8, except for a difference in the definition of variables. Eqs 5.24 and 5.25 have been computed and plotted in Figures 8 and 9.

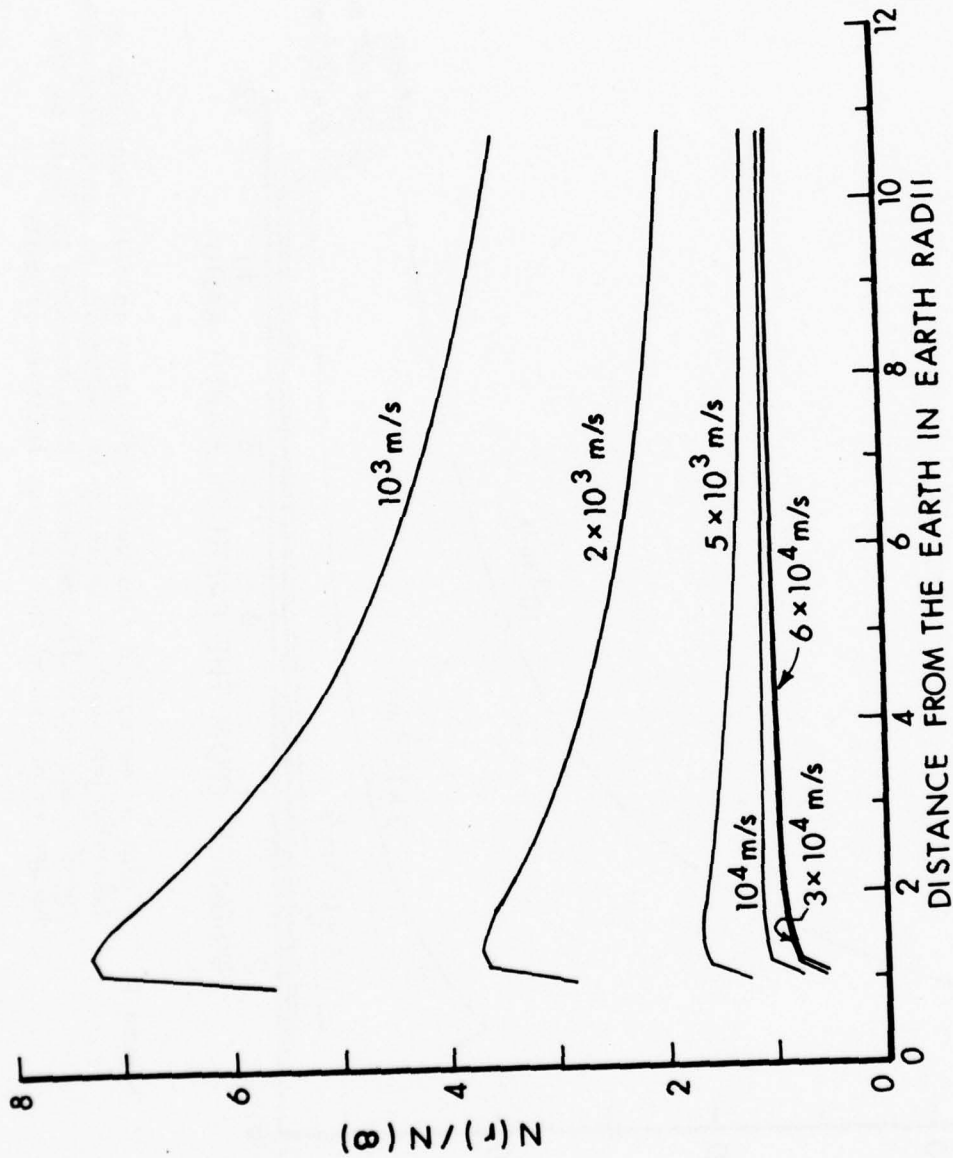


Figure 8. A plot of meteoroid number density versus distance from the earth measured in earth radii. At infinity the distribution is isotropic, uniform, and monoenergetic with speed U measured in units of escape velocity. The density at infinity is unity.

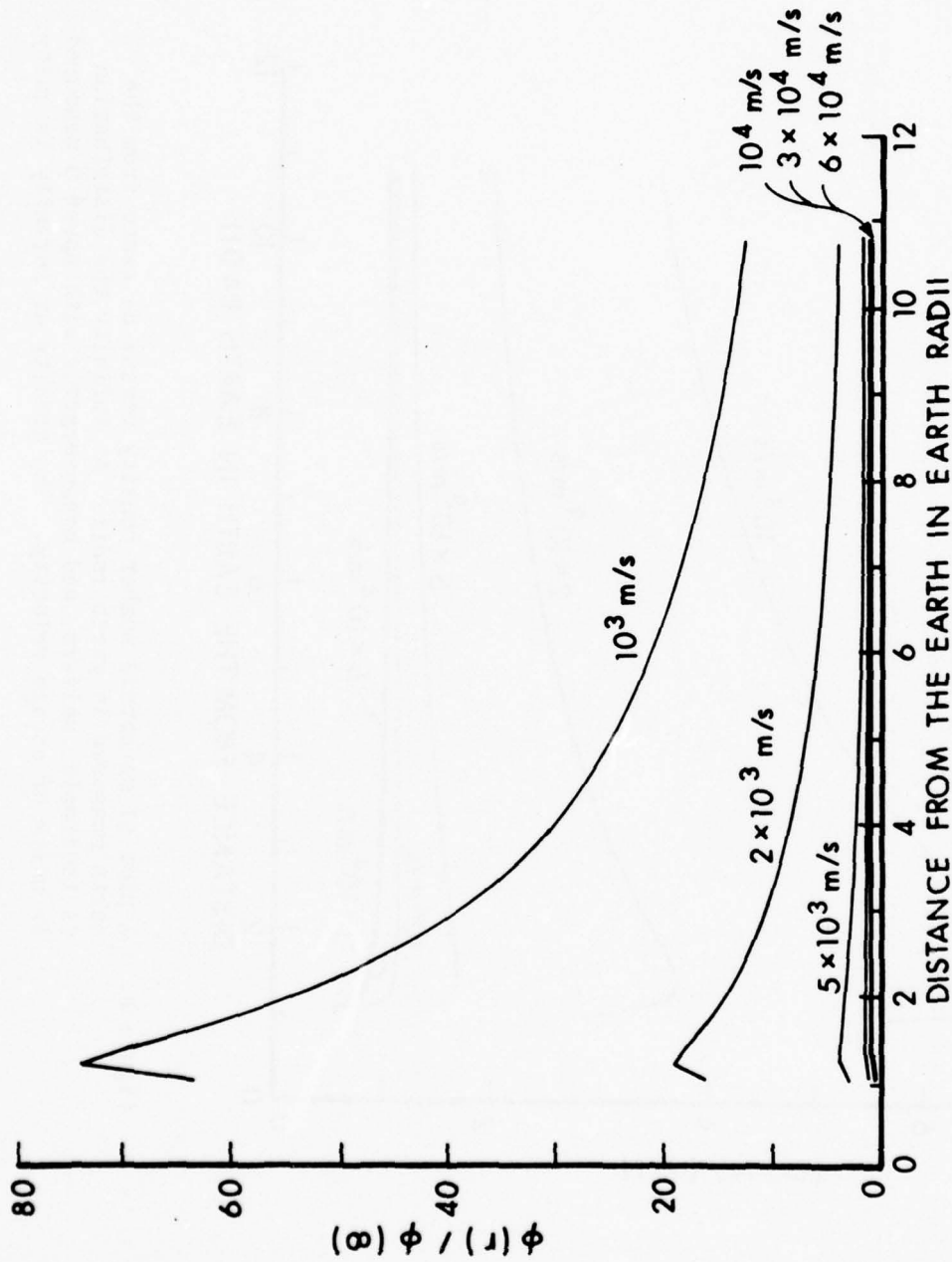


Figure 9. A plot of meteoroid flux versus distance in earth radii for a distribution which at infinity is isotropic, monoenergetic with speed U and spatially uniform. U is measured in units of the escape velocity and the flux at infinity is unity.

There have been speculations about populating various orbits with fragments as an anti-satellite measure. As a crude example, suppose that it is desired to put fragments into orbits from 100-300 miles above the earth in the zone extending to 20° latitudes north and south of the equator. The volume of this region is given by the formula

$$V = (4\pi/3)(r_2^3 - r_1^3) \cos \theta_0 = 1.7 \times 10^{20} \text{ M}^3, \quad 5.26$$

where r_2 is the outer radius, r_1 is the inner radius and θ_0 is the angular extent of the zone measured from the equator. If 10^6 particles are injected into a retrograde orbit so that they encounter the targets with maximum speed and flux, the speed of impact is roughly twice the orbital velocity or 15 km/sec. The impact rate is computed to be

$$\phi = N v = (10^6/1.7 \times 10^{20}) \times 16 \times 10^3 = 9.4 \times 10^{-11} \text{ p/m}^2 \text{ sec} \quad 5.27$$

or one impact on a square meter of surface in every 337 years. Thus it is seen that a cloud of projectiles is not an effective way to kill hostile satellites and that a chance encounter with debris left in space is vanishingly small, being about one in 1,000,000 years if we assume that 300 pieces are still in orbit.

A necessary condition for a particle to be injected into an orbit which misses the earth is, from Eq 5.13, that

$$R v(R) \leq R_i v(R_i) \sin \theta_m \quad 5.28$$

From the requirement that energy be conserved (Eqs 5.4 and 5.21),

$$v^2(R) - v_e^2 = v^2(R_i) - v_e^2 (R/R_i). \quad 5.29$$

From Eqs 5.28 and 5.29,

$$v^2(R_i) \geq [(R^2/R_i)(R_i - R)/R_i^2 \sin^2 \theta_m - R^2] v_e^2, \quad 5.30$$

which, when θ_m equals $\pi/2$, becomes

$$v^2(R_i) \geq [(R^2/R_i)/(R_i + R)] v_e^2. \quad 5.31$$

Thus we may write

$$v_e^2 (R^2/R_i)/(R_i + R) \leq v^2(R_i) \leq v_e^2 (R/R_i) . \quad 5.32$$

The quantity on the right is the escape velocity for a particle located a distance R_i from the earth. At 5 earth radii, for example, Eq 5.31 becomes

$$v_e/\sqrt{30} \leq v(R_i) \leq v_e/\sqrt{5} . \quad 5.33$$

6. MONOENERGETIC MONODIRECTIONAL FLOWS PAST A GRAVITATIONAL CENTER

If the earth should encounter a large loosely connected cloud of dust and meteoroids, it would appear to an observer on the earth that a stream of particles, with parallel trajectories at large distances on the approach to the earth, was flowing past the earth and being influenced by its gravitational field, as shown in Figure 10. Each particle orbit is characterized by a velocity v_∞ at large distances from the earth, an impact parameter "a", and an azimuthal angle ϕ . The impact parameter associated with a particle may be defined as the distance of closest approach of the particle to the center of the earth if the gravitational field were absent and the particle traveled in a straight line. A particle trajectory can be defined by the equations,^{3,4}

$$F \equiv r [1 + \epsilon \cos (\theta - \theta')] - B = 0 \quad 6.1$$

and
$$G \equiv \phi - \phi' = 0, \quad 6.2$$

where

$$B \equiv 2 a^2 v_\infty^2 / R v_e^2 \quad 6.3$$

and

$$\epsilon \equiv [1 + (4 a^2 v_\infty^4) / (R^2 v_e^4)]^{1/2}. \quad 6.4$$

and v_e is the escape velocity and R is the radius of the earth.

The constant θ' is defined by the requirement that r be infinite when θ takes on the values of zero and θ_m . From Eq 6.1 it follows that

$$\cos \theta' = (-1/\epsilon) = \cos (\theta_m - \theta') \quad 6.5$$

³George Joos, *Theoretical Physics*, Hafner Publishing Co., NY, 1950, p 89.

⁴Herbert Goldstein, *Classical Mechanics*, Addison Wesley Publishing Co., Inc., Reading, MA, 1959, p 77.

and that

$$\theta_m/2 = \theta' = \cos^{-1}(-1/\epsilon). \quad 6.6$$

If the definitions are made that

$$R = 1 \quad 6.7$$

and

$$U = v_\infty / v_e, \quad 6.8$$

Equations 6.3 and 6.4 can be written as

$$B = 2 a^2 U^2 \quad 6.9$$

and

$$\epsilon = [1 + 4 a^2 U^4]^{1/2}. \quad 6.10$$

The calculation of the vector current density $J(r, \theta)$ can proceed directly from the formalism leading to Eqs 3.10 and 3.14. If, for example, we identify the same particle flux through an element of area $a da d\phi$ at large distances to the left of Figure 10 and through an element of area $r^2 \sin\theta d\theta d\phi$ located at an arbitrary point (r, θ, ϕ) we can write the equation,

$$J_\infty a da d\phi = J(r, \theta) r^2 \sin\theta d\theta d\phi (\hat{r} \cdot \hat{t}). \quad 6.11$$

Since the Jacobian connecting the differential areas reduces to $\partial a / \partial \theta$, we can write

$$J(r, \theta) = [(J_\infty a) / (r^2 \sin\theta \cdot \hat{r} \cdot \hat{t})] (\partial a / \partial \theta). \quad 6.12$$

The vector scalar product $\hat{r} \cdot \hat{t}$ serves to project the area $\hat{r}(r^2 \sin\theta d\theta d\phi)$ onto a plane normal to the trajectory, the direction of which is defined by \hat{t} . In a like manner, by choosing a different element of area $\hat{\theta} r \sin\theta dr d\phi$, we can write,

$$J(r, \theta) = [(J_\infty a) / (r \sin\theta \cdot \hat{\theta} \cdot \hat{t})] (\partial a / \partial r). \quad 6.13$$

By combining Eqs 6.1, 6.5, 6.9 and 6.10, the values of "a" associated with a given r and θ can be found. Using the trigonometric identity,

$$\cos(\theta - \theta') = \cos\theta \cos\theta' + \sin\theta \sin\theta' \quad 6.14$$

we can use Eq 6.5 to write

$$\epsilon \cos(\theta - \theta') = -\cos\theta + (\epsilon^2 - 1)^{1/2} \sin\theta, \quad 6.15$$

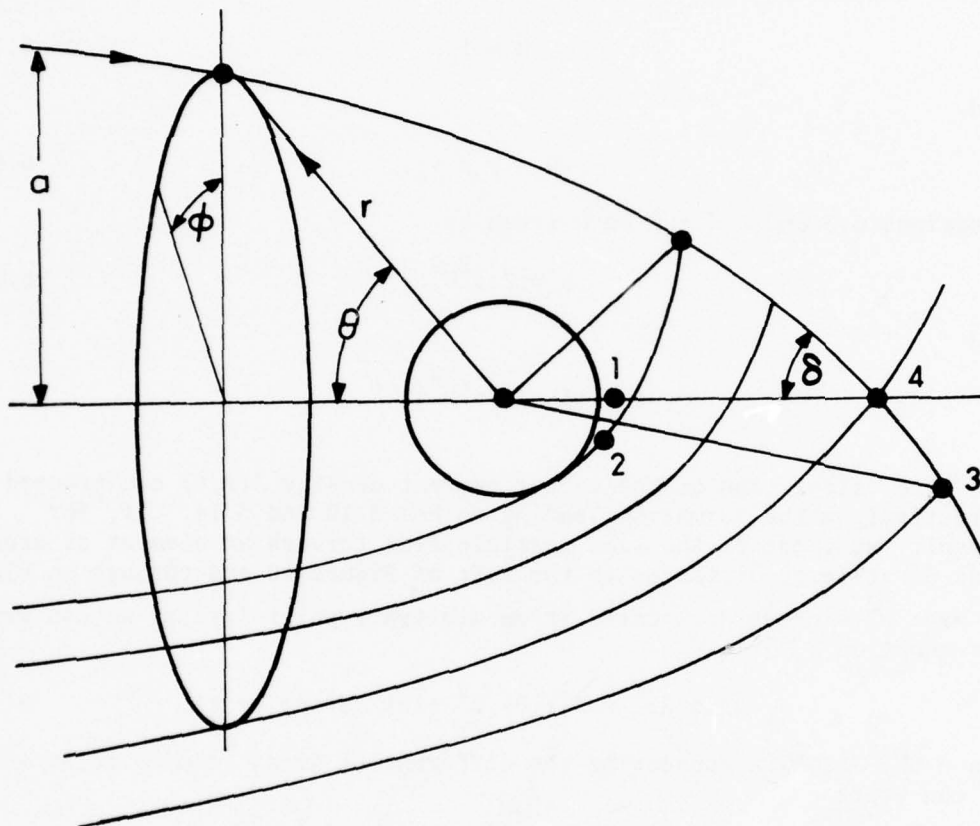


Figure 10. Flow of a parallel stream of meteoroids from left to right past the earth. Points (1) shielded by the earth will see no meteoroids. Some points (2) will receive from one direction, and other (3) will receive from two directions. Points along the symmetry axis (4) will receive from all directions lying on the cone defined by the angle δ .

where we have used the trigonometric identity,

$$\sin\theta' = (1 - \cos^2\theta')^{1/2} = (\epsilon^2 - 1)^{1/2}/\epsilon. \quad 6.16$$

Thus Eq 6.1, with the help of Eqs 6.9, 6.10 and 6.15 can be written as

$$r\{1 + [-\cos\theta + (\epsilon^2 - 1)^{1/2} \sin\theta] - 2 a^2 U^2\} = 0 \quad 6.17$$

or

$$r\{1 + [-\cos\theta + 2a U^2 \sin\theta] - 2 a^2 U^2\} = 0. \quad 6.18$$

This equation can be solved for "a" to yield the result,

$$a = (1/2)\{ r \sin\theta \pm [r^2 \sin^2\theta + 2r(1-\cos\theta)/U^2]^{1/2}\}. \quad 6.19$$

It follows that

$$\partial a / \partial r = (1/2) \left\{ \sin\theta + \frac{[r \sin^2\theta + (1-\cos\theta)/U^2]}{[r^2 \sin^2\theta + 2r(1-\cos\theta)/U^2]^{1/2}} \right\} \quad 6.20$$

and

$$\partial a / \partial \theta = (1/2) \left\{ r \cos\theta + \frac{[r^2 \sin\theta \cos\theta + (r \sin\theta)/U^2]}{[r^2 \sin^2\theta + 2r(1-\cos\theta)/U^2]^{1/2}} \right\}. \quad 6.21$$

By using our previous definition of \hat{t} as

$$\hat{t} = \bar{\nabla}F \times \bar{\nabla}G / |\bar{\nabla}F \times \bar{\nabla}G| \quad 6.22$$

Eqs 1 and 2 yield the result in spherical coordinates that

$$\bar{\nabla}F = \{-\hat{r}/r^2 + (\hat{\theta}/Br)\epsilon \sin(\theta-\theta')\} \quad 6.23$$

and

$$\bar{\nabla}G = \{[1/(r \sin\theta)]\hat{\phi}\}, \quad 6.24$$

so that

$$\hat{t} = [\hat{\theta}/r + (\hat{r}/B)\epsilon \sin(\theta-\theta')]/[1/r^2 + (\epsilon/B)^2 \sin^2(\theta-\theta')]^{1/2}. \quad 6.25$$

Thus

$$\hat{r} \cdot \hat{t} = [(\epsilon/B)\sin(\theta-\theta')]/[1/r^2 + (\epsilon/B)^2 \sin^2(\theta-\theta')]^{1/2} \quad 6.26$$

and

$$\hat{\theta} \cdot \hat{t} = [(1/r)]/[1/r^2 + (\epsilon/B)^2 \sin^2(\theta - \theta')]^{1/2}. \quad 6.27$$

where from Eqs 6.9 and 6.10

$$\epsilon/B = (1 + 4 a^2 U^4)^{1/2} / (2 a^2 U^2). \quad 6.28$$

Figure 11 illustrates the relationship of two trajectories which intersect at r and θ . The particle flux $\phi(r, \theta)$ at r and θ results from the sum of two flows, one associated with a_+ and the other with a_- , so that we can write

$$J(r, \theta) = |J_+(r, \theta)| + |J_-(r, 2\pi - \theta)| \quad 6.29$$

where $J_+(r, \theta)$, for example, is calculated from Eq 6.12 using the values of "a" and $\partial a / \partial \theta$ associated with the positive signs of Eqs 6.19 and 6.21 and the same value of "a" to compute ϵ/B of Eq 28 and $\hat{r} \cdot \hat{t}$ in Eq 6.26.

Because of shielding by the earth, $J_-(r, \theta)$ or both $J_+(r, \theta)$ and $J_-(r, \theta)$ may not reach a point. Trajectories with impact parameters less than that associated with a grazing trajectory will intersect the earth and fail to contribute to the particle flux thereafter. If

$$\theta < \theta' \quad 6.30$$

and

$$r > 1 \quad 6.31$$

the trajectory has not reached its closest approach to the earth. If

$$\theta > \theta' \quad 6.32$$

and

$$r_c < 1 \quad 6.33$$

where r_c is the point of closest approach, the flux contribution from that trajectory is zero.

The distance of closest approach r_c is easily calculated from the conservation of angular momentum and energy,

$$U a_g = U(1) \quad 6.34$$

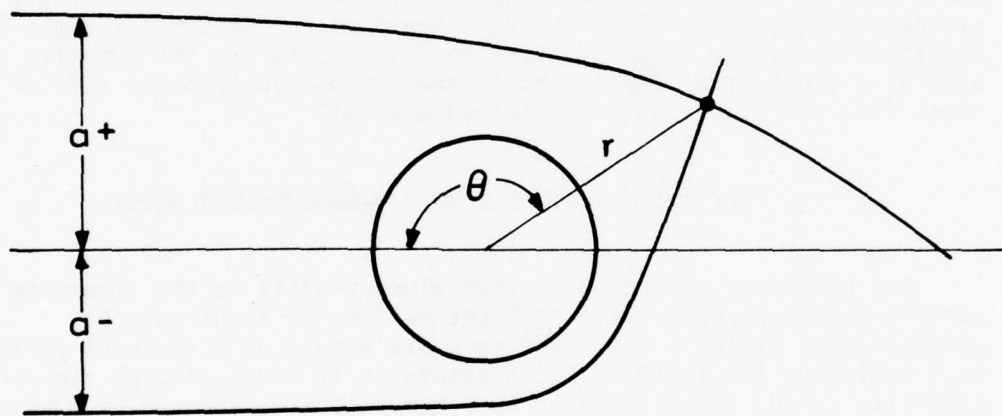


Figure 11. Two trajectories which intersect at r and θ . The values for a_+ and a_- are obtained from Eq 6.10.

and

$$U^2 = U^2(1) - 1, \quad 6.35$$

where the definition of Eqs 6.7 and 6.8 are used, $U(1)$ is the speed at the grazing point, and a_g is the impact parameter associated with a grazing trajectory. Eliminating $U(1)$ and solving for a_g we have the result,

$$a_g = (U^2 + 1)^{1/2}/U. \quad 6.36$$

Thus any trajectory with "a" less than " a_g " will intersect the earth. The tests and procedures for computing $\phi(r, \theta)$ are contained in Appendix 1. The isoflux plots for $\phi(r, \theta)$ are shown in Figures 12-14 for values of U equal to 0.5, 1 and 2. The infinite flux along the symmetry axis implies that, during a heavy meteor shower, it might be possible, under the right lighting conditions, to see the symmetry axis as a fluctuating light spot in the sky on the opposite side of the earth from the direction of meteoroid arrival.

7. FOCUSING OF PHOTONS BY A SCHWARZSCHILD FIELD

The preceding methods lend themselves readily to the treatment of stellar phenomena associated with the bending of light rays by gravitational fields. The light rays are viewed as a swarm of photons, each following its individual trajectory as it moves through the spherically symmetric field, first computed by Schwarzschild, created by a massive body. According to the general theory of relativity⁵, light rays passing by a massive celestial body are bent by an amount ψ according to the formula,

$$\psi = 4GM/ac^2 \equiv K/a \quad 7.1$$

where G is the universal gravitational constant, M is the mass of the body, usually considered to be a star, c is the velocity of light, and " a " is the impact parameter. It is conjectured, although it has never been observed, that an observer, in line with two stars as shown in Figure 15, will see the distant star magnified greatly by the lense effect of the Schwarzschild field associated with the nearer star.

⁵P. G. Bergmann, *Introduction to the Theory of Relativity*, Prentice Hall Inc., Englewood Cliffs, NJ, 1942, p 221.

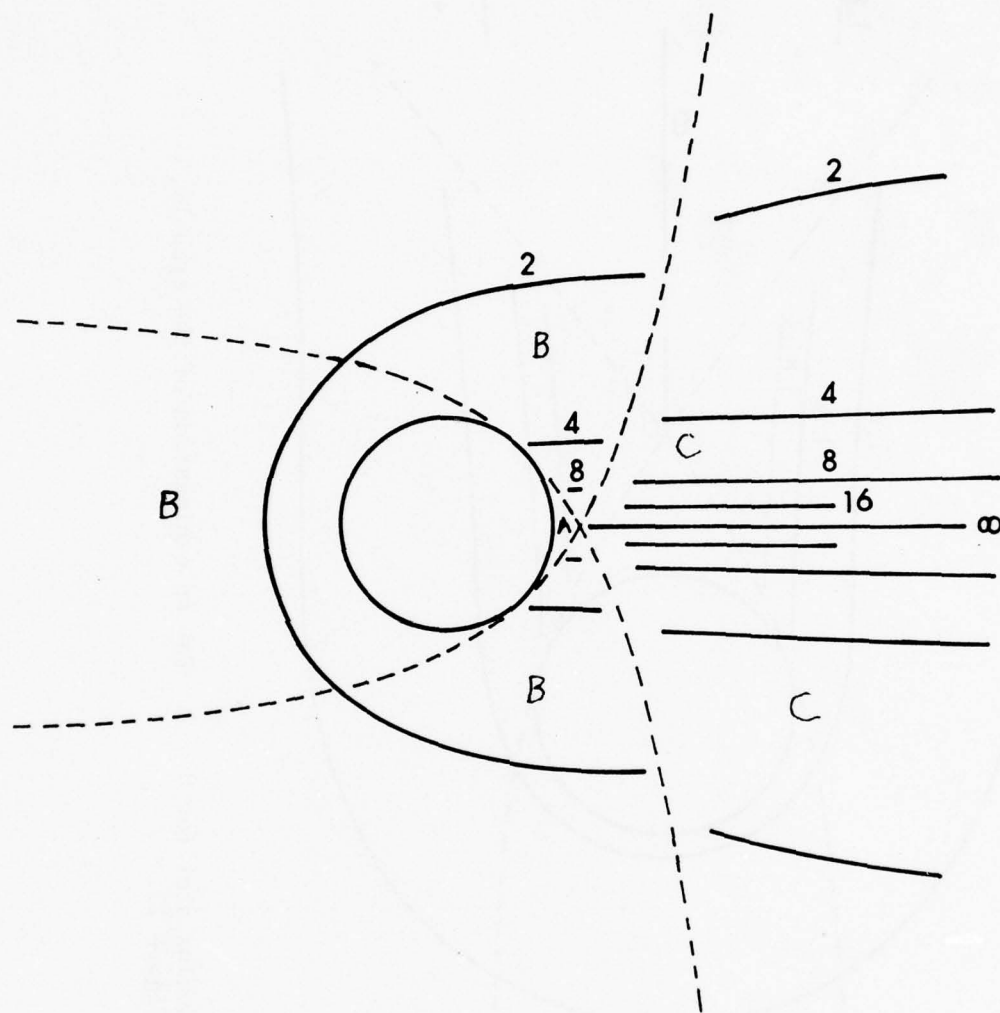


Figure 12. An isoflux plot for a parallel stream of meteoroids moving by the earth at half the escape velocity ($U = 1/2$). The dotted lines are grazing orbits, which demarcate the region A receiving no flux, the region B receiving flux in one direction, and the region C receiving flux in two directions. Intensities are calculated by assuming unit flux at infinity.

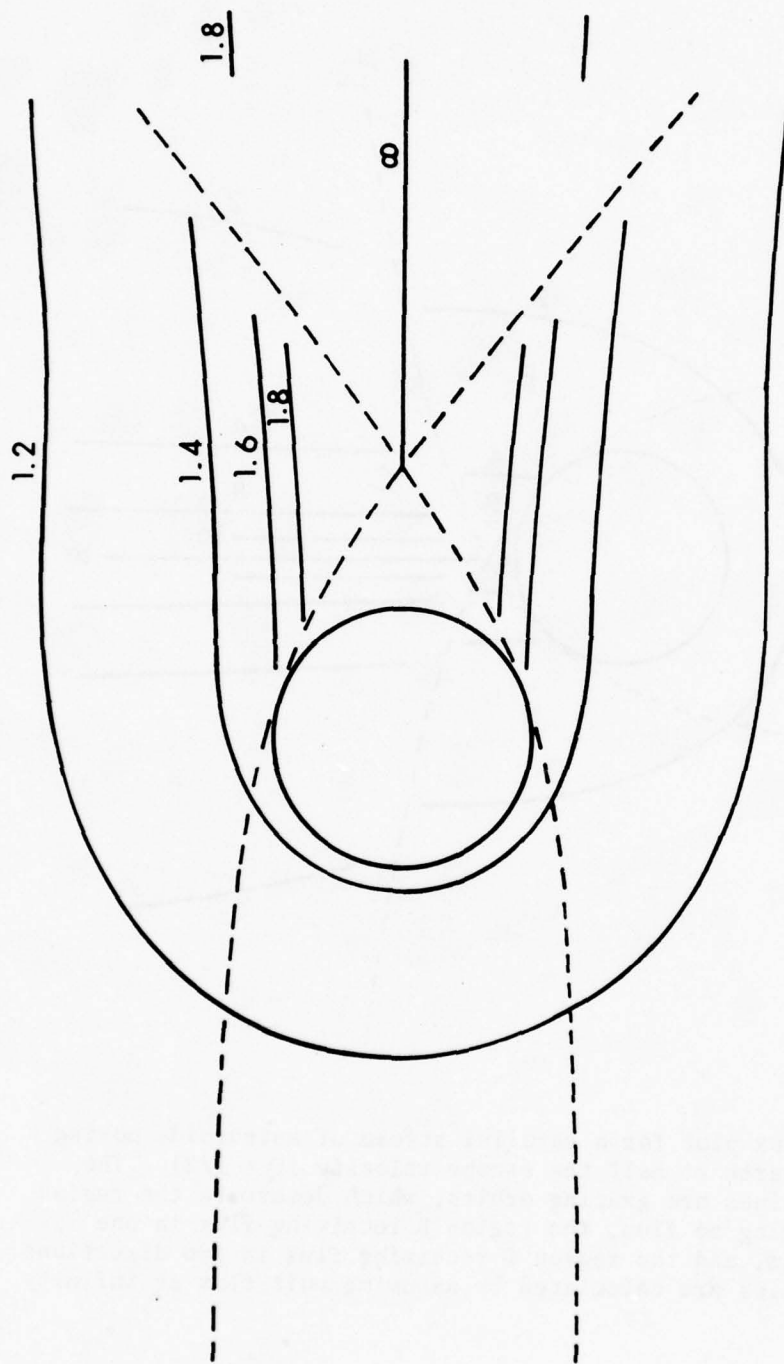


Figure 13. An isoflux plot for $U = 1$. For an explanation of the symbols, see Figure 12.

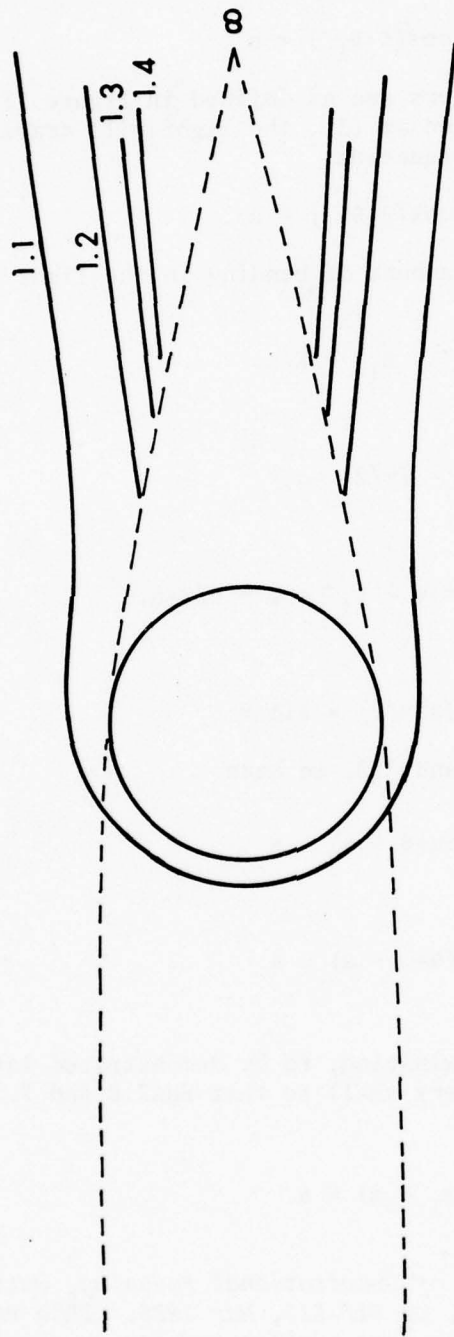


Figure 14. An isoflux plot for $U = 2$. For an explanation of the symbols, see Figure 12.

Light leaving the source at (1) in the direction in Figure 15 will travel in a direction defined by α according to the equation,⁶

$$r \cos(\theta - \theta_1') = a \quad 7.2$$

where the variables and parameters are as defined in Figure 15. After interaction with the star located at (3), the light will travel in a straight line according to the equation,

$$r \cos(\theta - \theta_2') = a \quad 7.3$$

From Eq 7.1 and Figure 15, the amount of bending in the light ray is given by the equation,

$$\psi = \theta_2' - \theta_1' = K/a \quad 7.4$$

Also, from Figure 15,

$$\theta_1' = (\pi/2) - \alpha, \quad 7.5$$

so that from Eqs 7.4 and 7.5,

$$\theta_2' = \psi + \theta_1' = \psi + \pi/2 - \alpha \quad 7.6$$

Using the identity that

$$\cos(x - \pi/2) = \sin x \quad 7.7$$

and Eqs 7.5 and 7.6 in Eqs 7.2 and 7.3, we have

$$r \sin(\theta + \alpha) = a \quad 7.8$$

and

$$r \sin(\theta - \psi + \alpha) = a \quad 7.9$$

We will now make the approximation, to be demonstrated later, that $\alpha, \beta, \psi, \theta, \theta_1'$ and $\pi - \theta_2'$ are very small so that Eqs 7.8 and 7.9 can be written as

$$r_1(\theta_1' + \alpha) = a \quad 7.10$$

⁶ Guy Mayer, *Collective Features of Gravitational Focusing, Optics Communications, Vol. 16, No. 3, pp 317-319, Mar 1976. This reference takes an optical approach to the same problem and has an excellent bibliography on light focusing by gravitational fields.*

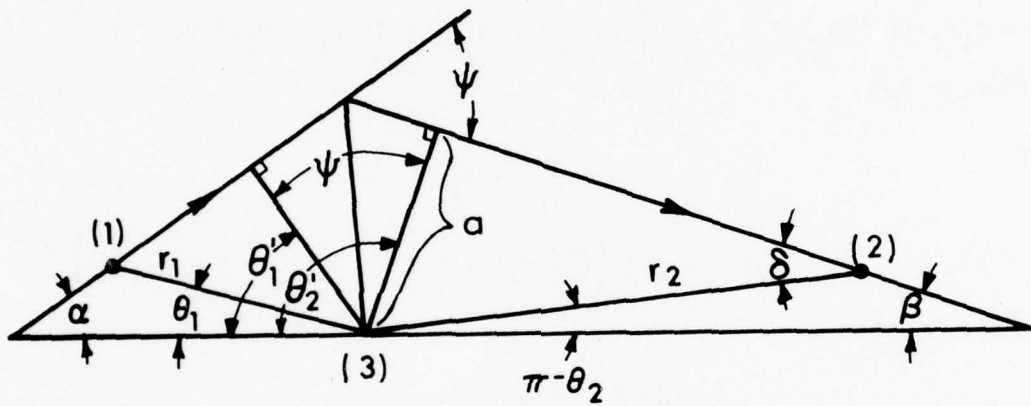


Figure 15. The lense effect associated with gravitational fields. The observer at (2) sees light from a distant star at (1) focused by a nearer star at (3) so that the star at (1) appears magnified and distorted. The angles are greatly exaggerated. The rays arriving at (2) from sources at (1) and (3) have an apparent angular separation δ .

and

$$r_2(\pi - \theta_2 + \psi - \alpha) = a \quad 7.11$$

where the identity,

$$\sin x = \sin(\pi - x), \quad 7.12$$

has been used to obtain Eq 7.11 from Eq 7.9. The subscripts 1 and 2 have been introduced to designate the incoming and outgoing rays. Eqs 7.4, 7.10 and 7.11 can be used to solve for a and α . From them,

$$a = r_1 r_2 \{ [(\pi - \theta_2) + \theta_1] \pm \left([(\pi - \theta_2) + \theta_1]^2 + 4K(r_1 + r_2)/(r_1 r_2) \right)^{1/2} \} / [2(r_1 + r_2)] \quad 7.13$$

and

$$\alpha = \frac{a}{r_1} - \theta_1 \quad 7.14$$

$$= -\theta_1 + r_2 \{ [(\pi - \theta_2) + \theta_1] \pm \left([(\pi - \theta_2) + \theta_1]^2 + 4K(r_1 + r_2)/(r_1 r_2) \right)^{1/2} \} / [2(r_1 + r_2)]$$

$$- \frac{\partial \alpha}{\partial \theta_2} = + \frac{r_2}{2(r_1 + r_2)} \pm \frac{[(\pi - \theta_2) + \theta_1] r_2}{2(r_1 + r_2) \{ [(\pi - \theta_2) + \theta_1]^2 + 4K(r_1 + r_2)/(r_1 r_2) \}^{1/2}} \quad 7.15$$

For our purposes we will assume that r_1 and r_2 are equal to r so that Eqs 7.14 and 7.15 reduce to the equations,

$$\alpha = -\theta_1 + (1/4) \{ [(\pi - \theta_2) + \theta_1] \pm \left([(\pi - \theta_2) + \theta_1]^2 + 8K/r \right)^{1/2} \} \quad 7.16$$

and

$$- \frac{\partial \alpha}{\partial \theta_2} = \frac{1}{4} \pm \frac{1}{4} \frac{[(\pi - \theta_2) + \theta_1]}{([(\pi - \theta_2) + \theta_1]^2 + 8K/r)^{1/2}} \quad 7.17$$

From Figure 15,

$$r_2 \sin \delta = a, \quad 7.18$$

and from Eqs 7.3 and 7.6,

$$r_2 \cos [\theta_2 - \psi - (\pi/2) + \alpha] = r_2 \sin[\theta_2 - \psi + \alpha] = a. \quad 7.19$$

From the identity of Eq 7.12, Eq 7.19 can be written in the form

$$r_2 \sin[\pi - \theta_2 + \psi - \alpha] = a. \quad 7.20$$

Thus, comparing Eqs 7.18 and 7.20,

$$\delta = \pi - \theta_2 + \psi - \alpha. \quad 7.21$$

Using Eqs 7.4 and 7.14,

$$\delta = (\pi - \theta_2) + K/[r_1(\theta_1 + \alpha)] - \alpha, \quad 7.22$$

where α is given by Eq 7.14 or 7.16.

The angle δ given by Eq 7.22 is the apparent angular separation of light arriving from point sources of light (stars) located at point (1), (r_1, θ_1) , and point (3), the coordinate origin, of Figure 15. To appreciate the optics of the gravitational field, it is useful to calculate the distortion of the circular stellar disc and to compute the relative intensity of various parts of the image from the point of view of the observer at point (2) of Figure 15.

To perform the first task, the stellar image is depicted as shown in Figure 16. The angles θ_1 and ϕ_1 associated with an emission from the point P on the circumference of the stellar disc, are related to the angular displacement of the star θ_0 and the rotation angle ϕ by the equations

$$\cot \phi_1 = (\theta_0/\theta) \csc \phi - \cot \phi \quad 7.23$$

and

$$\theta_1 = \theta \sin \phi / \sin \phi_1 \quad 7.24$$

where θ is the angle subtended by the radius of the stellar disc. Because the trajectories lie in a plane, ϕ_1 and ϕ_2 are equal, and we can use the value of θ_1 in Eqs 7.16 and 7.21 to compute two values of δ for each value of θ_1 .

Suppose in Figure 15 that θ_1 is zero and that the star at point (1) emits an amount light $S \sin \alpha \, d\alpha \, d\phi$ into the element of solid angle $\sin \alpha \, d\alpha \, d\phi$. Assume that this light arrives at point (2) so that an amount of light $J(\bar{r}_2) \hat{n} \cdot \hat{t} \, r_2^2 \sin \theta_2 \, d\theta_2 \, d\phi$ passes through the element of area $r_2^2 \sin \theta_2 \, d\theta_2 \, d\phi$. Equating these two expressions we have

$$J(\bar{r}_2)/S = (\sin \alpha / \hat{n} \cdot \hat{t} \, r_2^2 \sin \theta_2) (\partial \alpha / \partial \theta_2) \quad 7.25$$

We can assume that α and $\pi - \theta_2$ are very small and that $\hat{n} \cdot \hat{t}$ is unity so that we have

$$J(\bar{r}_2)/S = \{ \alpha / [r_2^2 (\pi - \theta_2)] \} (\partial \alpha / \partial \theta_2) \quad 7.26$$

The radiation directly from the star, using the inverse square law, would be given by the equation,

$$J(\bar{r}_2)/S = 1 / [(2r)^2] = 1 / (4r^2) \quad 7.27$$

assuming that r_1 and r_2 are equal to r .

We could rotate the diagram of Figure 15 by an angle $-\theta_1$ about point (3) without changing the physical relationships involving r_1 , r_2 , a , and ψ . Thus Eq 7.26 should be applicable to the more general condition of Figure 15 if we replace $\pi - \theta_2$ everywhere by $[(\pi - \theta_2) + \theta_1]$. As expected, "a" calculated by Eq 7.13 is unchanged by this rotation. Although α is changed by the rotation ($-\theta_1$) according to Eq 7.14, $\partial \alpha / \partial \theta_2$ is a function only of $[(\pi - \theta_2) + \theta_1]$ as expected, since the intensity of light at (r_2, θ_2) , as given by Eq 7.26, must be independent of the choice of coordinate system. We therefore modify Eq 7.26 to read

$$J(\bar{r}_2)/S = \{ (\alpha + \theta_1) / [r_2^2 (\pi - \theta_2 + \theta_1)] \} (\partial \alpha / \partial \theta_2) \quad 7.28$$

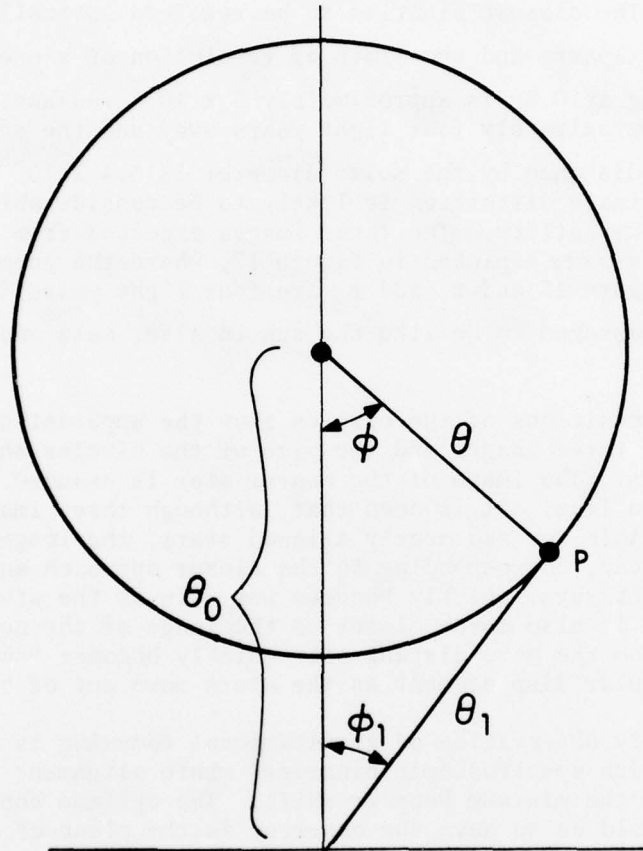


Figure 16. Description of the stellar disc in terms of angular displacements. The relationships of Eqs 7.23 and 7.24 are easily obtained by noting that $\theta_0 = \theta \cos \phi + \theta_1 \cos \phi_1$ and that $\theta \sin \phi = \theta_1 \sin \phi_1$. These two equations can be solved for θ_1 and ϕ_1 .

We are now in a position to discuss what an observer should see as two stars are approximately aligned. Eqs 7.23 and 7.24 permit us to pick an arbitrary point on the circumference of the more distant star and to compute its angular displacement from the nearer star by means of Eq 7.22. Equation 7.28 permits us to compute the intensity of light from that point. The closest binaries to be resolved optically⁷ are 7.7×10^{-6} radians apart, and the limit of resolution of a one meter telescope operating at 0.5μ is approximately 5×10^{-7} radians. The nearest star is approximately four light years away and the angle subtended at that distance by the solar diameter is 3.4×10^{-8} radians. Therefore stellar image distortion is likely to be considerably beyond our observational capability. The three images expected from a nearly aligned pair of stars are depicted in Figure 17, where the geometry is described by Figure 15 and r_1 and r_2 are four light years in distance. The two stars are assumed to be like the sun in size, mass and light emission.

The vertical positions of the circles show the apparent angular separations of the three images and the size of the circles show the relative brightness. The image of the nearer star is assumed to be on the horizontal zero line. It is seen that, although three images are theoretically possible for two nearly aligned stars, the image from the more distant star, corresponding to the closer approach and greater bending of the light rays, quickly becomes very dim as the stars move out of alignment. It also moves closer to the image of the nearer star. The other image from the more distant star quickly becomes "normal" in brightness and angular displacement as the stars move out of alignment.

The most likely observation of gravitational focusing is likely to be associated with spectroscopic binaries, where alignment should be coincident with the minimum Doppler shift. The optimum conditions for observation would be to have the observer in the plane of revolution of two stars which are coupled closely enough gravitationally to have a reasonably short period of revolution. One star should be big and bright and the other should be more massive but very small to avoid occlusion of too much light. The requirements for alignment, close association, and differences in type of star will of course eliminate most observed spectral binaries, but it would be interesting to search for one which would verify gravitational focusing.

⁷ E. A. Fath, *The Elements of Astronomy*, 4th Edition, McGraw-Hill Book Co., New York & London, 1944, p 284.

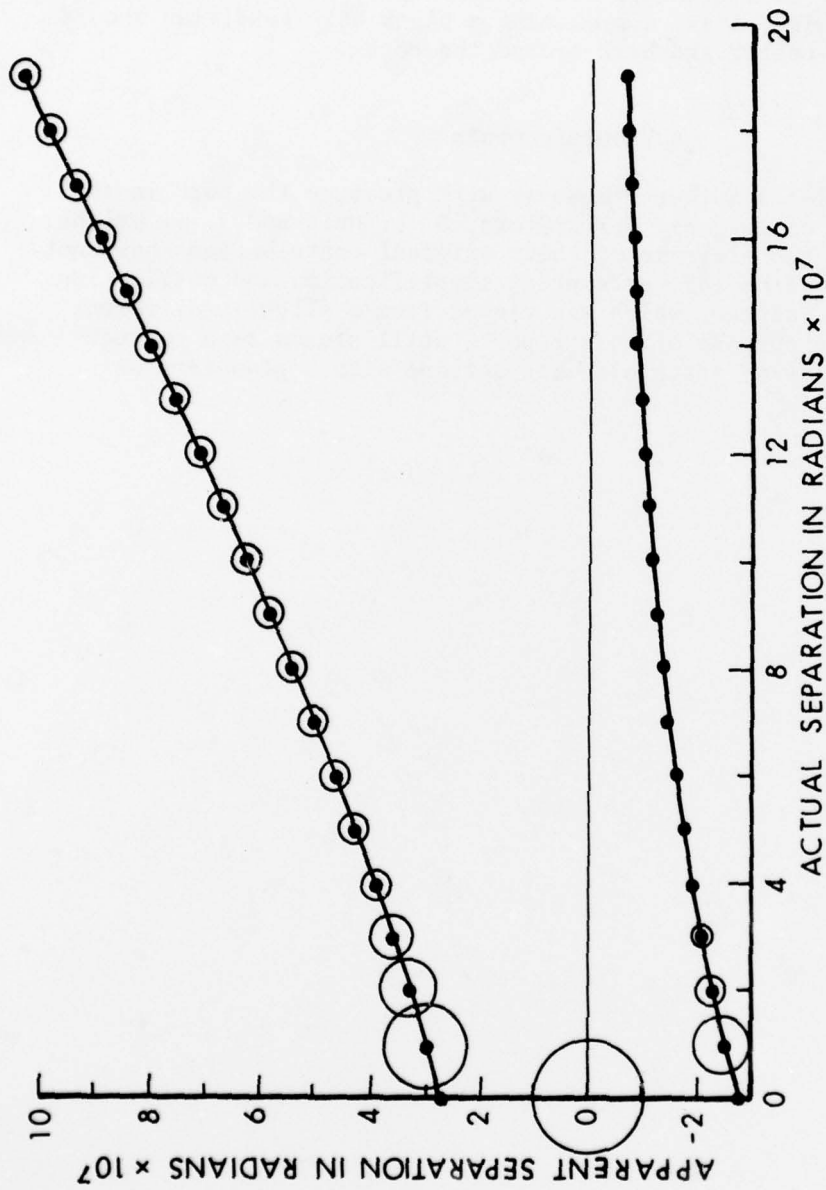


Figure 17. A depiction of what an observer sees as two stars move out of line. The vertical positions of the circles show the apparent angular separation of the three images and the sizes show the relative brightness. The nearer star is assumed to be on the horizontal zero line. It is clear that, although three images are theoretically possible, the third image is usually very dim. Thus optical binaries will look like optical binaries except in unusual circumstances.

Massive galaxies with dense star clusters at the center should show limb darkening and center brightening because of gravitational light focussing, but without resolution of individual stars, the effect could not be attributed with certainty to gravitational focussing. Likewise, stars approaching a black hole condition should be bright in the center and dark around the edges.

Acknowledgements

The first listed author remembers with pleasure the work in this area with former colleagues, H. E. Stern, D. P. Hale and J. J. Wright. It is hoped that the elegance of their original contributions have not suffered too much from this attempt at simplification and unification. The work of S. F. Singer, which was viewed from a slightly different viewpoint for the purpose of this report, still stands as a correct and elegant summary of meteoroid interactions with a planetary or stellar field.

REFERENCES

1. S. F. Singer, *Nature*, Oct 78, 1961, pp 321-323.
2. R. D. Shelton, et al, *Astronomical Journal* 70 No. 2, Mar 1965, pp 166-170.
3. George Joos, *Theoretical Physics*, Hafner Publishing Co., NY, 1950, p 89.
4. Herbert Goldstein, *Classical Mechanics*, Addison Wesley Publishing Co., Inc., Reading, MA, 1959, p 77.
5. P. G. Bergmann, *Introduction to the Theory of Relativity*, Prentice Hall Inc., Englewood Cliffs, NJ, 1942, p 221.
6. Guy Mayer, *Collective Features of Gravitational Focusing*, *Optics Communications*, Vol. 16, No. 3, pp 317-319, Mar 1976.
7. E. A. Fath, *The Elements of Astronomy*, 4th Edition, McGraw-Hill Book Co., New York & London, 1944, p 284.

APPENDIX 1

Procedure for Computing $\phi(r, \theta)$.

Formulae

$$\phi(r, \theta) = |J(r, \theta, a_+)| + |J(r, \theta, a_-)| \quad 1$$

$$a = (1/2) \{ r \sin \theta + [r^2 \sin^2 \theta + 2r(1 - \cos \theta)/U^2]^{1/2} \} \quad 2$$

$$\frac{\partial a}{\partial \theta} = (1/2) \left\{ r \cos \theta + \frac{[r^2 \sin \theta \cos \theta + r \sin \theta / U^2]}{[r^2 \sin^2 \theta + 2r(1 - \cos \theta)/U^2]^{1/2}} \right\} \quad 3$$

$$\frac{\partial a}{\partial r} = (1/2) \left\{ \sin \theta + \frac{[r \sin^2 \theta + (1 - \cos \theta)/U^2]}{[r^2 \sin^2 \theta + 2r(1 - \cos \theta)/U^2]^{1/2}} \right\} \quad 4$$

$$\epsilon = (1 + 4 a^2 U^4)^{1/2} \quad 5$$

$$B = 2 a^2 U^2 \quad 6$$

$$\theta' = \cos^{-1} (-1/\epsilon) \quad 7$$

$$J(r, \theta, a) = [a / (r^2 \sin \theta \cdot \hat{r} \cdot \hat{t})] (\partial a / \partial \theta) \quad 8$$

$$J(r, \theta, a) = [a / (r \sin \theta \cdot \hat{\theta} \cdot \hat{t})] (\partial a / \partial r) \quad 9$$

$$\hat{r} \cdot \hat{t} = [(\epsilon/B) \sin(\theta - \theta')] / [1/r^2 + (\epsilon/B)^2 \sin^2(\theta - \theta')]^{1/2} \quad 10$$

$$\hat{\theta} \cdot \hat{t} = [1/r] / [1/r^2 + (\epsilon/B)^2 \sin^2(\theta - \theta')]^{1/2} \quad 11$$

$$a_g = (U^2 + 1)^{1/2} / U \quad 12$$

Procedure

1. Choose r, θ , and U , $1 < r < \infty$, $0 < \theta < 2\pi$, $0 < U < \infty$.
2. Compute $|a_+|$ and $|a_-|$. (Eq 2).
3. Compute θ' (Eqs 5 and 7) for $|a_+|$ and $|a_-|$. These values are labeled θ'_+ and θ'_- .
4. Compute $(\partial a / \partial \theta)_+$ and $(\partial a / \partial \theta)_-$ (Eq 3). Use θ for $(\partial a / \partial \theta)_+$ and $(2\pi - \theta)$ in place of θ in calculating $(\partial a / \partial \theta)_-$.
5. Compute $(\hat{r} \cdot \hat{t})_+$ and $(\hat{r} \cdot \hat{t})_-$ (Eq 10). Use θ for $(\hat{r} \cdot \hat{t})_+$ and $(2\pi - \theta)$ for θ in $(\hat{r} \cdot \hat{t})_-$.
6. Compute a_g (Eq 12).
7. Compute $|J(r, \theta, a_+)|$ from Eq 8 using $|a_+|$, $(\partial a / \partial \theta)_+$ and $(\hat{r} \cdot \hat{t})_+$ as calculated above. Set $|J(r, \theta, a_+)|$ equal to zero for $\theta > \theta'_+$ and $a_+ < a_g$.
8. Compute $|J(r, \theta, a_-)|$ from Eq 8 using $|a_-|$, $(\partial a / \partial \theta)_-$ and $(\hat{r} \cdot \hat{t})_-$ as calculated above. Set $|J(r, \theta, a_-)|$ equal to zero for $a_- < a_g$.
9. Compute $\phi(r, \theta)$ from Eq 1.
10. If $\hat{r} \cdot \hat{t} = 0$ above, use Eq 4 and 11 in Eq 9, using the same general procedure as before.

APPENDIX 2

Computation of Apparent Stellar Brightness and Image Distortion Caused by Gravitational (Schwarzschild) Bending of Light Rays

The physical constants assumed for the calculation are listed in Table A2-1. From Eq 7.1 and the constants of Table A2-1 we see that a grazing orbit is bent by an amount of 9×10^{-8} radians. The subtended angle of the nearer star is 3.35×10^{-8} radians. The formulae used for the calculation are listed in Table A2-2. The procedures for the calculation are listed in Table A2-3.

Table A2-1

Physical Constants Assumed for the Calculation

$G = 6.67 \times 10^{-11}$ (S.I.) = Universal Gravitational Constant

$C = 3 \times 10^8$ m/sec = Velocity of light

$M = 2 \times 10^{30}$ kg = Mass of sun

$r_1 = r_2 = 4 \times 10^{16}$ m = Distances from star 1 to
star 2 to observer

$k = 4GM/C^2 = 6000$ m

$R = 6.7 \times 10^8$ m = Radius of Sun

Table A2-2

Formulae Used for Computations

$$a_{\pm} = (r/4) \{(\pi - \theta_2)_{\pm} [(\pi - \theta_2)_{\pm}^2 + 8k/r]^{1/2}\} \quad 1$$

$$\alpha_{\pm} = (a_{\pm}) r_2 \quad 2$$

$$- \frac{\partial \alpha}{\partial \theta_2} = (1/4)_{\pm} (1/4) [(\pi - \theta_2)] / [(\pi - \theta_2)_{\pm}^2 + 8k/r]^{1/2} \quad 3$$

$$\psi_{\pm} = k/a_{\pm} \quad 4$$

$$\delta_{\pm} = (\pi - \theta_2) + \psi_{\pm} - \alpha_{\pm} \quad 5$$

$$J_{\pm}(r) r^2/S = |[\alpha_{\pm}/(\pi - \theta_2)] (\partial \alpha_{\pm} / \partial \theta_2)| \quad 6$$

Table A2-3

Procedures for Calculations

1. Compute a_+ and a_- from Eq 1., $0 < \pi - \theta_2 < 10^{-5}$.
2. Compute α_+ and α_- from Eq 2, using a_+ to calculate α_+ , etc.
3. Compute $|(\partial\alpha/\partial\theta_2)_+|$ and $|(\partial\alpha/\partial\theta_2)_-|$ from Eq 3.
4. Compute ψ_+ and ψ_- from Eq 4.
5. Compute δ_+ and δ_- from Eq 5.
6. Compute $J_+(r)r^2/S$ and $J_-(r)r^2/S$ from Eq 6.
7. Plot δ_+ and δ_- versus $\pi - \theta_2$ and label each point with the value of $J_+(r)r^2/S$ and $J_-(r)r^2/S$ as appropriate.

DISTRIBUTION LIST

<u>No. of Copies</u>	<u>Organization</u>	<u>No. of Copies</u>	<u>Organization</u>
12	Commander Defense Documentation Center ATTN: DDC-DDA Cameron Station Alexandria, VA 22314	1	Commander US Army Electronics Research and Development Command Technical Support Activity ATTN: DELSD-L Fort Monmouth, NJ 07703
1	Commander US Army Materiel Development and Readiness Command ATTN: DRCDMD-ST 5001 Eisenhower Avenue Alexandria, VA 22333	2	Commander US Army Missile Research and Development Command ATTN: DRDMI-R DRDMI-YDL Redstone Arsenal, AL 35809
2	Commander US Army Armament Research and Development Command ATTN: DRDAR-TSS Dover, NJ 07801	1	Commander US Army Tank Automotive Rsch and Development Command ATTN: DRDTA-UL Warren, MI 48090
1	Commander US Army Armament Materiel Readiness Command ATTN: DRSAR-LEP-L, Tech Lib Rock Island, IL 61299	1	Director US Army TRADOC Systems Analysis Activity ATTN: ATAA-SL, Tech Lib White Sands Missile Range NM 88002
1	Commander US Army Aviation Research and Development Command ATTN: DRSAV-E 12th and Spruce Streets St. Louis, MO 63166	<u>Aberdeen Proving Ground</u>	
1	Director US Army Air Mobility Research and Development Laboratory Ames Research Center Moffett Field, CA 94035	Dir, USAMSAA ATTN: DRXSY DRXSY-MP, H. Cohen Cdr, USATECOM ATTN: DRSTE-TO-F Cdr, USACSL, EA ATTN: ATSL-CLC, Bldg E1570 Dr. Tom Welch Dir, Wpns Sys Concepts Team Bldg. E3516, EA ATTN: DRDAR-ACW	
1	Commander US Army Communications Rsch and Development Command ATTN: DRDCO-PPA-SA Fort Monmouth, NJ 07703		

USER EVALUATION OF REPORT

Please take a few minutes to answer the questions below; tear out this sheet and return it to Director, US Army Ballistic Research Laboratory, ARRADCOM, ATTN: DRDAR-TSB, Aberdeen Proving Ground, Maryland 21005. Your comments will provide us with information for improving future reports.

1. BRL Report Number _____

2. Does this report satisfy a need? (Comment on purpose, related project, or other area of interest for which report will be used.)

3. How, specifically, is the report being used? (Information source, design data or procedure, management procedure, source of ideas, etc.) _____

4. Has the information in this report led to any quantitative savings as far as man-hours/contract dollars saved, operating costs avoided, efficiencies achieved, etc.? If so, please elaborate.

5. General Comments (Indicate what you think should be changed to make this report and future reports of this type more responsive to your needs, more usable, improve readability, etc.) _____

6. If you would like to be contacted by the personnel who prepared this report to raise specific questions or discuss the topic, please fill in the following information.

Name: _____

Telephone Number: _____

Organization Address: _____

